Intensity Fluctuations in the Output of cw Laser Oscillators. I

D. E. McCUMBER
Bell Telephone Laboratories, Murray Hill, New Jersey
(Received 29 March 1965; revised manuscript received 10 September 1965)

Using linearized rate equations, we have calculated the intensity fluctuations expected in the output of four-level cw laser oscillators. Intrinsic quantum effects have been included by restricting the eigenvalues of photon and atomic population operators to discrete integral values and by using equivalent noise sources. The total output fluctuations increase monotonically with output power; the *relative* fluctuations decrease monotonically, and at high output levels inversely as the output power squared. The low-frequency fluctuations differ in that the relative fluctuations increase with output below threshold (noise amplifier region) but decrease sharply above threshold (dynamic saturation region). Curves typical of gas, solid, and diode lasers are illustrated. The theory agrees well with preliminary experimental results.

1. INTRODUCTION

IN single-mode operation continuous-wave (cw) laser oscillators are characterized by an output spectrum having a narrow but finite width. It has been recognized[1] that, as in more conventional oscillators,[2] this residual width results primarily from frequency (or phase) modulation by noise and that at high power levels amplitude (or intensity) modulation by noise contributes insignificantly. The suppression of amplitude or intensity fluctuations in the high-power oscillator is intimately connected with the nonlinear saturation mechanism which determines the operating power level of the laser.[3] Below the oscillation threshold or in the extreme wings of the spectral line this saturation mechanism is inoperative (in the latter case because of time constants in the saturation process), and noise phase modulation and noise amplitude modulation are comparable. In this paper we indicate correlation experiments which can be used to verify the amplitude stability of cw lasers and compute the amplitude fluctuations expected in four-level lasers having negligible population in the lower laser level. In a subsequent paper (II) we shall discuss the amplitude stability of systems which have significant lower-level populations, and in a later paper (III) we shall indicate jointly with M. Lax how the rate-equation results of the first two papers follow as limiting cases from a more general analysis of laser noise. Although the rate-equation method does fail for fluctuation frequencies exceeding the homogeneous atomic or cavity linewidths,[4] it obtains over the frequency range for which intensity fluctuations are most important. Moreover, it has an inherent physical simplicity which it is useful to exploit. High-frequency corrections will be computed in Paper III.

Our present results differ from those of the Van der Pol model used by Haus[5,6] and others primarily through our inclusion of the *dynamic* (rather than instantaneous) response of the atomic populations to changes in laser intensity. This difference, which is less important in gas lasers than in solid or diode lasers, is responsible for "spiking" resonances which have been observed experimentally[7,8] and which are discussed in Sec. 6 below. A detailed examination of the Van der Pol model will be postponed to Paper III.

For mathematical simplicity we assume in this paper that on the time scale of interest, the atomic spectral line is homogeneously broadened and that in multimode lasers the population rate-equations can be linearized about spatially uniform atomic populations. Although these assumptions encompass a large class of lasers, especially if coupling parameters are adjusted to compensate known inhomogeneities, phenomena which depend explicitly upon the existence of such inhomogeneities will not be adequately represented. Examples are the Lamb dip in gas lasers[9] and mode locking in lasers having three or more excited modes spaced uniformly in frequency. To include such phenomena accurately, a more detailed treatment along lines previously charted by Lamb[3] will be required.

A complete statistical description of the output of a laser oscillator requires the specification of an infinite sequence of field correlation functions[10]

$$G_n(x_1,\cdots,x_n;x_1',\cdots,x_n') = \langle E^{(-)}(x_1)\cdots E^{(-)}(x_n)E^{(+)}(x_n')\cdots E^{(+)}(x_1')\rangle, \quad (1.1)$$

where $E^{(+)}(x)$ and $E^{(-)}(x)$ are, respectively, the positive-frequency and negative-frequency electric-field operators at the space-time point $x=(\mathbf{r},t)$. In a second-quantization formalism $E^{(+)}(x)$, when acting on states

[1] J. P. Gordon, H. J. Zeiger, and C. H. Townes, Phys. Rev. **99**, 1264 (1955); J. P. Gordon, J. Res. Natl. Bur. Std. (U. S.) **68D**, 1031 (1964).
[2] A. Blaquière, Ann. Radioelec. **8**, 36 (1953); **8**, 153 (1953); W. A. Edson, Proc. IEEE **48**, 1544 (1960); J. A. Mullen, *ibid.* **48**, 1467; M. J. E. Golay, *ibid.* **48**, 1473.
[3] W. E. Lamb, Jr., Phys. Rev. **134**, A1429 (1965).
[4] D. E. McCumber, Phys. Rev. **130**, 675 (1963).
[5] H. A. Haus, J. Quantum Electronics **1**, 179 (1965).
[6] C. Freed and H. A. Haus, Appl. Phys. Letters **6**, 85 (1965).
[7] J. E. Geusic, in *Proceedings of the Physics of Quantum Electronics Conference, San Juan, Puerto Rico, 1965*, edited by P. L. Kelley, B. Lax, and P. E. Tannenwald (McGraw-Hill Book Company, Inc., New York, 1965).
[8] N. Bloembergen and S. Dimitrewsky (private communication).
[9] R. A. McFarlane, W. R. Benett, and W. E. Lamb, Appl. Phys. Letters **2**, 189 (1963); A. Szöke and A. Javan, Phys. Rev. Letters **10**, 521 (1963).
[10] R. J. Glauber, Phys. Rev. **130**, 2529 (1963).

to its right, is a photon annihilation operator, and $E^{(-)}(x)=E^{(+)}(x)^+$ is the corresponding creation operator.[10] The simplest correlation function $G_1(x_1; x_1')$ relates to the spectrum measured by familiar dispersion or diffraction spectrometers.[4,11,12] As we have noted, the finite width of this spectrum for laser oscillators results primarily from frequency or phase modulation induced by noise. The theory of measurement of more general functions (1.1) has been discussed in detail by many authors.[12–15]

An important subclass of the correlation functions (1.1) is the set of intensity correlation functions

$$F_n(x_1,\cdots,x_n)=G_n(x_1,\cdots,x_n; x_1,\cdots,x_n), \quad (1.2)$$

which relate field intensities $I(x)=E^{(-)}(x)E^{(+)}(x)$ at different points. Such correlation functions can be measured by correlating (with appropriate time delays) the output of n photomultipliers or similar intensity-measuring devices.[12–14,16] They also relate to the moments $\langle N^m\rangle$ of the number N of photons measured in some fixed interval T at any one detector.[15,17] In what follows we shall be concerned with the simplest intensity correlation function $F_2(x_1,x_2)$.

Apparatus useful for the measurement of this function have been described by Hanbury Brown and Twiss,[18] by Rebka and Pound,[19] and by other authors.[6,7,20–24] Hanbury Brown and Twiss (HB&T) correlate the intensities measured by two separate photomultipliers in an extremely stable linear multiplier. To within the frequency-response limitations of the components, its output gives $F_2(x_1,x_2)$ directly. The power spectrum or Fourier transform of $F_2(x_1,x_2)$ can alternatively be obtained by frequency analyzing the output from a single detector[6,7,24]; however, in this case the desired information is superimposed upon shot noise and internal detector noise.[18] In the two-detector HB&T system the uncorrelated detector and shot noises of the separate detectors average to zero in the final output. Rebka and Pound[19] and others[20–23] measure the function $F_2(x_1,x_2)$ indirectly by counting coincidences in the production of photoelectrons by a pair of photomultipliers. The useful information is here superimposed upon the average number of chance coincidences which would occur if the emission of photoelectrons in the two photomultipliers was completely random.

Although shot and detector noises average to zero in the HB&T method, there are instantaneous noise fluctuations in the output from the linear multiplier. The intrinsic signal-to-noise ratios of the HB&T and coincidence methods are comparable; however, an upper bound on the counting rate imposed by the requirements of multiple-coincidence resolution limits the coincidence method in practice to systems in which the correlation effects are relatively strong.[18] HB&T have used their apparatus with considerable success to measure the very weak correlations in radiation from broad-band stellar sources. For strong sources for which shot noise is less of a problem, it is often practicable to use the simpler single-detector system.[6,7,24]

If $I_j(t)$ is the field intensity at the jth photomultiplier ($j=1$ or 2) and if the real function $B_j(t)$ is the intensity-impulse response function for that detector and its subsequent electronics, then the output signal from detector channel j is

$$J_j(t)=\int_{-\infty}^{t} dt' B_j(t-t')I_j(t'). \quad (1.3)$$

The different apparatus described above all measure various properties of the output correlation function

$$C_0(\tau)=\langle J_1(t+\tau)J_2(t)\rangle_t, \quad (1.4)$$

where $\langle\ \rangle_t$ denotes a time average. In the single-detector system $J_1(t)=J_2(t)$.

In order to express $C_0(\tau)$ in terms of the intensity correlation function

$$C_I(\tau)=\langle I_1(t+\tau)I_2(t)\rangle_t, \quad (1.5)$$

a special case of the function $F_2(x_1,x_2)$, it is convenient to introduce the power spectra or Fourier transforms of the correlation functions (1.4) and (1.5). Typically,

$$P_I(\omega)=\int_{-\infty}^{\infty} d\tau\, e^{i\omega\tau}C_I(\tau), \quad (1.6a)$$

$$C_I(\tau)=\int_{-\infty}^{\infty} \frac{d\omega}{2\pi} e^{-i\omega\tau}P_I(\omega). \quad (1.6b)$$

---

[11] M. Born and E. Wolf, *Principles of Optics* (Pergamon Press, Inc., New York, 1959), Chap. X.

[12] L. Mandel and E. Wolf, Rev. Mod. Phys. **37**, 231 (1965).

[13] R. J. Glauber, in *Quantum Optics and Electronics*, edited by C. DeWitt, A. Blandin, and C. Cohen-Tannoudji (Gordon and Breach Science Publishers, Inc., New York, 1965), p. 63.

[14] M. L. Goldberger, H. W. Lewis, and K. M. Watson, Phys. Rev. **132**, 2764 (1963).

[15] P. L. Kelley and W. H. Kleiner, Phys. Rev. **136**, A316 (1964).

[16] For simplicity we use "photomultiplier" as the generic term for all such detectors.

[17] L. Mandel, Phys. Rev. **136**, B1221 (1964).

[18] R. Hanbury Brown and R. Q. Twiss, Proc. Roy. Soc. (London) **242A**, 300 (1957); **243A**, 291 (1958). The first article contains an interesting discussion of the role of quantum uncertainties in correlation measurements.

[19] G. A. Rebka and R. V. Pound, Nature **180**, 1035 (1957).

[20] R. Q. Twiss and A. G. Little, Australian J. Phys. **12**, 77 (1959).

[21] A. Adám, L. Jánossy, and P. Varga, Acta Phys. Hungarica **4**, 301 (1955); E. Brannen and H. I. S. Ferguson, Nature **178**, 481 (1956).

[22] J. A. Armstrong and A. W. Smith, Phys. Rev. Letters **14**, 68, 208 (1965).

[23] A. W. Smith and J. A. Armstrong, Phys. Letters **16**, 38 (1965); J. A. Armstrong and A. W. Smith, Phys. Rev. **140**, A155 (1965).

[24] L. J. Prescott and A. Van der Ziel, Phys. Letters **12**, 317 (1964). This letter contains a basic error in interpretation; properly used [$G<(R_1R_2)^{-1/2}$], Eq. (1) does not describe the dependence of the results upon pumping strength even qualitatively.

If we also introduce the frequency response function

$$b_j(\omega)=\int_0^\infty dt\, e^{i\omega t}B_j(t)=b_j(-\omega)^*, \tag{1.7}$$

which is the Fourier-Laplace transform of the impulse response function $B_j(t)$ of Eq. (1.3), then it is easy to demonstrate[18] that

$$P_0(\omega)=b_1(\omega)b_2(\omega)^*P_I(\omega). \tag{1.8}$$

For notational brevity we assume that the two detector channels are identical: $b_1(\omega)b_2(\omega)^*=|b(\omega)|^2$.

In the limit $|\tau|\to\infty$ the field intensities on the right-hand side of Eq. (1.5) are uncorrelated:

$$C_I(\tau)\xrightarrow[|\tau|\to\infty]{} C_I(\infty)=\langle I_1(t)\rangle_t\langle I_2(t)\rangle_t. \tag{1.9}$$

Subtracting this constant from $C_I(\tau)$, we obtain a function

$$\Delta C_I(\tau)=C_I(\tau)-C_I(\infty), \tag{1.10}$$

which describes the nontrivial intensity correlations and whose power spectrum

$$\Delta P_I(\omega)=\int_{-\infty}^\infty d\tau\, e^{i\omega\tau}\Delta C_I(\tau) \tag{1.11a}$$

$$=P_I(\omega)-2\pi C_I(\infty)\delta(\omega) \tag{1.11b}$$

is a smooth function of ω. Using this spectrum in (1.8), we see that the output correlation function (1.4) is

$$C_0(\tau)=|b(0)|^2C_I(\infty)+\int_{-\infty}^\infty \frac{d\omega}{2\pi}e^{-i\omega\tau}|b(\omega)|^2\Delta P_I(\omega). \tag{1.12}$$

If $b(0)=0$, as is easily arranged, the first term on the right-hand side of (1.12) will vanish and $C_0(\tau)=\Delta C_0(\tau)$.

If in the HB&T apparatus the signal from channel 2 is delayed a time τ relative to that from channel 1, the average output from the linear multiplier and its subsequent integrating circuit is precisely the correlation function (1.4) or (1.12).

If in the coincidence method τ_R is the coincidence resolving time and τ is the relative delay time of the two input channels,[19–23] the counting rate is proportional to

$$C_C(\tau,\tau_R)=\int_{-\tau_R}^{\tau_R}[d\tau'\, C_I(\tau+\tau') \tag{1.13a}$$

$$=2\tau_RC_I(\infty)+2\tau_R\int_{-\infty}^\infty \frac{d\omega}{2\pi}e^{-i\omega\tau}\frac{\sin\omega\tau_R}{\omega\tau_R}\Delta P_I(\omega). \tag{1.13b}$$

It is sometimes useful to interpret the coincidence experiments in terms of an intensity correlation time τ_I defined by the equation[18,25]

$$\tau_I=\int_{-\infty}^\infty d\tau\,\Delta C_I(\tau)/C_I(\infty)=\Delta P_I(0)/C_I(\infty). \tag{1.14}$$

If the coincidence resolving time τ_R is long compared with τ_I (poor resolution),[26] we see from Eqs. (1.13) and (1.14) that the ratio

$$C_C(0,\tau_R)/C_C(\infty,\tau_R)=1+\tau_I/2\tau_R \tag{1.15a}$$

gives a direct measure of τ_I. In the opposite limit of high resolution ($\tau_R\ll\tau_I$), this ratio is

$$C_C(0,\tau_R)/C_C(\infty,\tau_R)=1+\Delta C_I(0)/C_I(\infty), \tag{1.15b}$$

independent of both τ_R and τ_I.

To interpret the single-detector measurements, it is useful to assume that the impulse response function $B_j(t)$ of Eq. (1.3) describes the "shot" response to a single detected quantum (photon) of the radiation field. If $\Delta P_I(\omega)$ represents the power spectrum of the intrinsic intensity correlations, as it does in the preceding two-detector systems, the single-detector method measures the power spectrum[18,27]

$$\Delta P_I(\omega)\Big|_{\substack{\text{single}\\ \text{detector}}}=|b(\omega)|^2[\eta\langle I(t)\rangle_t+\eta^2\Delta P_I(\omega)], \tag{1.16a}$$

where η is the detector quantum efficiency and $\langle I(t)\rangle_t$ is the average incident intensity in photons per second. The latter rate can be determined from the average dc output from the detector, which is

$$\langle J(t)\rangle_t=|b(0)|\,\eta\langle I(t)\rangle_t. \tag{1.16b}$$

If in the single-detector method the frequency analyzer passes signal components whose frequencies lie in the narrow frequency bands $f_0-\frac{1}{2}\Delta f<|f|<f_0+\frac{1}{2}\Delta f$, $\Delta f\ll f_0$, the root-mean-square output from the frequency analyzer is ($\omega=2\pi f$)

$$\mathrm{rms}(f_0)=\left\{\int_{|f|\in(f_0\pm\frac{1}{2}\Delta f)}\frac{d\omega}{2\pi}\Delta P_0(\omega)\Big|_{\substack{\text{single}\\ \text{detector}}}\right\}^{1/2} \tag{1.17a}$$

$$=(2\Delta f)^{1/2}|b(2\pi f_0)|\{\eta\langle I(t)\rangle_t+\eta^2\Delta P_I(2\pi f_0)\}^{1/2}, \tag{1.17b}$$

if $\Delta P_I(\omega)$ and $b(\omega)$ do not vary significantly over the interval Δf.

Just as it is convenient to avoid calibration difficulties in the coincidence method by measuring the dimensionless ratio (1.15), it is also convenient in the single-detector method to measure $\Delta P_I(\omega)$ relative to shot noise.[6,7,24] For this purpose it is useful to know that, if the radiation from a black-body thermal source tra-

[25] E. M. Purcell, Nature **178**, 1449 (1956).

[26] More precisely, Eq. (1.15a) obtains when $\Delta P_I(\omega)\approx\Delta P_I(0)$ for all $|\omega|\lesssim\tau_R^{-1}$.

[27] S. O. Rice, Bell System Tech. J. **23**, 282 (1944); **24**, 46 (1945).

verses an ideal passive filter which transmits only in Lorentz-shaped lines centered about the optical frequencies $\pm\nu_0$ and having full width $\Delta\nu \ll \nu_0$, then the intensity-fluctuation power spectrum $\Delta P_I(\omega)$ is[28]

$$\Delta P_I(\omega)\Big|_{\substack{\text{black-body;}\\ \text{Lorentzian}}} = \langle I(t)\rangle_t^2 \frac{4\pi\Delta\nu}{\omega^2+(2\pi\Delta\nu)^2}. \quad (1.18)$$

In the broad-band limit $\Delta\nu \gg f_0$ and in the limit of weak intensity $\langle I(t)\rangle_t \to 0$ or low quantum efficiency $\eta \to 0$, shot noise will dominate the single-detector measurement (1.17). This fact suggests[24] that in single-detector measurements on an unknown source one measures for each frequency f_0 both the frequency-analyzer output rms(f_0) and the average detector output $\langle J(t)\rangle_t$. If one then adjusts the intensity of a broad-band black-body source so as to reproduce the output rms(f_0) and measures the corresponding average detector output, it follows immediately from the preceding expressions that

$$\langle J(t)\rangle_t\Big|_{\substack{\text{broad-band}\\ \text{source}}} = \langle J(t)\rangle_t + \eta^2 |b(0)|\, \Delta P_I(2\pi f_0), \quad (1.19a)$$

where the quantities on the right-hand side refer to the unknown. Equivalently,

$$\frac{\Delta P_I(2\pi f_0)}{C_I(\infty)} = \frac{|b(0)|}{\langle J(t)\rangle_t^2} \times \left[\langle J(t)\rangle_t\Big|_{\substack{\text{broad-band}\\ \text{source}}} - \langle J(t)\rangle_t\right]. \quad (1.19b)$$

In the following sections we compute the intensity correlation function $\Delta C_I(\tau)$ or, equivalently, its power spectrum $\Delta P_I(\omega)$ for simple models of a four-level steady-state laser oscillator perturbed by noise. The noise sources most relevant to amplitude or intensity fluctuations (in contradistinction to frequency or phase fluctuations, which we do not consider here) are (i) quantum noise and (ii) pump fluctuations. Because $h\nu \gg kT$ in lasers, thermal noise is not important. Population pulsations, driven by beating optical fields,[3] can also modulate the intensity spectra of multimode lasers, and this effect is discussed further in Sec. 4.

In lasers having a single photon mode λ, the intensity power spectra (1.6) and (1.11) reflect the time development of the photon number operator $b_\lambda^\dagger b_\lambda$, where b_λ and $b_\lambda^\dagger$ are the usual annihilation and creation operators describing the electromagnetic field: $[b_\lambda, b_\lambda] = 0$, $[b_\lambda, b_\lambda^\dagger] = 1$. If the width of the intensity-modulation spectrum $\Delta P_I(\omega)$ is less than the homogeneous atomic and cavity linewidths and if nonresonant components are neglected,[29] the time development of $b_\lambda^\dagger b_\lambda(t)$ can be described by rate equations which only involve electromagnetic field operators in the combination $b_\lambda^\dagger b_\lambda(t)$—that is, which only involve diagonal elements of the photon density matrix. In Sec. 2 we base our analysis of single-mode lasers upon such rate equations quantized in the manner of Shimoda, Takahasi, and Townes by restricting the eigenvalues of photon and atomic population operators to discrete integral values.[30] Unquantized rate equations were developed for lasers by Statz and DeMars[31] and have been used for the analysis of laser transients by several authors. A review is given by Kleinman.[32]

Using the results of Sec. 2 as a guide, we develop in Sec. 3 a convenient Langevin model with white-noise sources which, when used with the unquantized rate equations, reproduce the Shimoda, Takahasi, and Townes quantum effects. The mathematical simplifications of this model permit us to extend the single-mode results of Sec. 2 to multimode cavities in Sec. 4 and to general pumping schemes in Sec. 5. In treating multimode lasers, we use modified rate equations which involve electromagnetic field operators in the bilinear combinations $b_\lambda^\dagger b_\nu(t)$— that is, which involve off-diagonal as well as diagonal elements of the photon density matrix. Our treatment correctly predicts population pulsations, but it does not lead to mode locking.[3]

In the final section, Sec. 6, we summarize our principal results and discuss numerical examples for typical lasers. Readers not interested in the details of special cases or in derivations may turn directly to this last section after reading the first few paragraphs of Sec. 2, especially Eqs. (2.1)–(2.3) and (2.12), where the important laser parameters are defined.

---

[28] A representative derivation is contained in Refs. 18. In the range $|\omega| \ll 2\pi\Delta\nu$ the magnitude of the spectrum (1.18) varies inversely as $\Delta\nu$. We wish to emphasize that this is a special property of the black-body thermal source whose features enter the HB&T analysis in the assumption of random phases for the different frequency components of the Fourier decomposition of the electromagnetic field. That the random-phase assumption is equivalent to the assumption of a normal or Gaussian distribution for the electromagnetic field (appropriate to a thermal-equilibrium distribution of the field in a *hohlraum*) follows from the central limit theorem of statistics [H. Cramér, *Mathematical Methods of Statistics* (Princeton University Press, Princeton, New Jersey, 1946)]. The random-phase assumption does not apply, for example, to spectra which derive their width from frequency modulation. Laser sources display the $1/\Delta\nu$ dependence below threshold; above threshold saturation stabilizes the intensity and modifies the simple $1/\Delta\nu$ dependence.

[29] Similar assumptions have been used by Lamb, Ref. 3, Eqs. (38) and (70).

[30] K. Shimoda, H. Takahasi, and C. H. Townes, Proc. Phys. Soc. Japan **12**, 686 (1957).

[31] H. Statz and G. DeMars, in *Quantum Electronics*, edited by C. H. Townes (Columbia University Press, New York, 1960), p. 530.

[32] D. A. Kleinman, Bell System Tech. J. 43, 1505 (1964). The parameters of Sec. 2 become in Kleinman's notation $\pi_\lambda = 1/t_m$, $\gamma_\lambda = 1/t_p$, and $\Gamma_2 = 1/t_r$. In typical systems $\pi_\lambda \ll \gamma_\lambda$, Γ_2; this fact is used in our analysis. If the relaxation from level 2 to level 1 in the system of Fig. 1 is primarily by spontaneous emission, then [Kleinman, Eq. (7)]

$$\pi_\lambda^{-1} = (8\pi\nu^2 n_{\text{ref}}^3/c^3) V t_r \Delta\nu,$$

where t_r is the spontaneous-emission lifetime, n_{ref} is the index of refraction, V is the cavity volume, and $\Delta\nu$ is the width of the frequency-ν atomic line. Formulas of this type are generally valid only if $\pi_\lambda t_r \ll 1$.

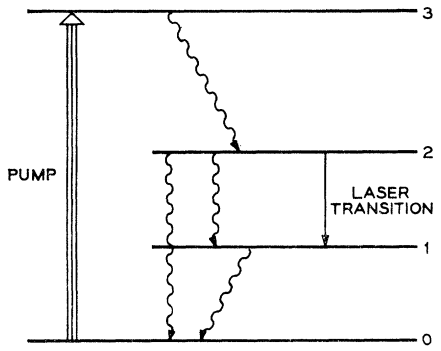

FIG. 1. Atomic energy levels of prototype four-level laser. Pump excites ground-state atoms to level 3 from which they quickly decay incoherently to upper-laser-level 2. Atoms in this level decay by emitting laser photons (solid line) or by other incoherent processes (wavy lines). The lower-laser-level 1 depopulates rapidly to the ground state.

2. FOUR-LEVEL LASER, SINGLE PHOTON MODE

Consider initially the prototype four-level laser of Fig. 1. For simplicity, assume that the average level populations $N_1(t)=N_3(t)=0$ and that $N_0(t)\approx N_T$, the total number of active atoms in the laser cavity. Also assume that the cavity is resonant at only a single photon mode λ and that the average number of photons in that mode is $P_\lambda(t)$. If $R(t)$ is the rate at which ground-state atoms are excited to the upper laser level by the pump and if $N_2(t)-N_1(t)=N_2(t)$ is the atomic inversion, rate-equations describing population changes with increasing time are[31,32]

$$(\partial/\partial t)N_2(t)=R(t)-\Gamma_2N_2(t)-\pi_\lambda[1+P_\lambda(t)]N_2(t), \quad (2.1a)$$

$$(\partial/\partial t)P_\lambda(t)=s(t)+\pi_\lambda[1+P_\lambda(t)]N_2(t)-\gamma_\lambda P_\lambda(t). \quad (2.1b)$$

Here π_λ, the *mode* rate,[32] is the average rate for spontaneous emission into the laser mode, Γ_2 is the average rate of decay from the upper laser level by other than laser-photon emission, and γ_λ is the average rate of decay of photon number in the undriven laser cavity. The term $s(t)$ is a small noise signal to be described further below and in Sec. 3.

If $\bar{P}_\lambda$, $\bar{N}_2$, and $\bar{R}$ are the time-averaged values of $P_\lambda(t)$, $N_2(t)$, and $R(t)$ in steady-state operation, then Eqs. (2.1) imply [average value of $s(t)$ vanishes]

$$\bar{R}=\Gamma_2\bar{N}_2+\pi_\lambda(1+\bar{P}_\lambda)\bar{N}_2, \quad (2.2a)$$

$$\gamma_\lambda\bar{P}_\lambda=\pi_\lambda(1+\bar{P}_\lambda)\bar{N}_2. \quad (2.2b)$$

If $p_\lambda(t)$, $n_2(t)$, and $r(t)$ are small fluctuations of $P_\lambda(t)=\bar{P}_\lambda+p_\lambda(t)$, etc., about these average values, then to first order in the small fluctuations Eqs. (2.1) give

$$(\partial/\partial t)n_2(t)=r(t)-[\Gamma_2+\pi_\lambda(1+\bar{P}_\lambda)]n_2(t)-\pi_\lambda\bar{N}_2p_\lambda(t), \quad (2.3a)$$

$$(\partial/\partial t)p_\lambda(t)=s(t)+\pi_\lambda(1+\bar{P}_\lambda)n_2(t)-(\gamma_\lambda-\pi_\lambda\bar{N}_2)p_\lambda(t). \quad (2.3b)$$

Above threshold where nonlinear saturation effects are important, the fluctuations are known experimentally to constitute only a small modulation of the steady-state output, and Eqs. (2.3) adequately approximate Eqs. (2.1). (Systems having intense "spiking" in their outputs[32] are, of course, exceptions and are excluded from our analysis.) Below threshold the relative fluctuations may be large; however, the nonlinear terms in Eqs. (2.1) are then small, so that the linear approximation does not generate significant errors. In the immediate vicinity of threshold the errors may be more significant,[33] but we shall use the linear Eqs. (2.3) for want of a better tractable approximation.

Shimoda, Takahasi, and Townes (STT)[30] have emphasized that the eigenvalues of the photon number operator $b_\lambda^\dagger b_\lambda$ and of corresponding atomic population operators $a_m^\dagger a_m$ are not continuous variables but are constrained by quantum mechanics to integral values. This constraint is important to our analysis because it is the source of quantum shot noise. Following STT, we introduce the probability $P(n,p;t)$ that at time t the level-2 atomic population and the mode-λ photon population, respectively, have the integral values (n,p) in an ensemble of identically prepared systems. Under the conditions for which Eqs. (2.1) were derived, this probability is governed for increasing time t by the differential equation

$$\begin{aligned}(\partial/\partial t)P(n,p;t)&=R(t)P(n-1,p;t)\\&+\Gamma_2(n+1)P(n+1,p;t)+s(t)P(n,p-1;t)\\&+\gamma_\lambda(p+1)P(n,p+1;t)+\pi_\lambda(n+1)pP(n+1,p-1;t)\\&-[R(t)+\Gamma_2n+s(t)+\gamma_\lambda p+\pi_\lambda n(p+1)]P(n,p;t),\end{aligned} \quad (2.4)$$

plus initial conditions. Summing Eq. (2.4) over admissible values of (n,p), we correctly find that the total probability is a constant of the motion.

The probabilities $P(n,p;t)$ can be viewed as diagonal elements of the ensemble density matrix. It is not necessary to introduce supplemental off-diagonal elements, because such elements play no role in Eqs. (2.1)–(2.4). However, off-diagonal elements are relevant to multimode systems, and they will be mentioned again in Sec. 4.

Multiplying Eq. (2.4) by n and summing over (n,p), we obtain Eq. (2.1a):

$$(\partial/\partial t)N_2(t)=R(t)-\Gamma_2N_2(t)-\pi_\lambda\textstyle\sum_{np}n(p+1)P(n,p;t) \quad (2.5a)$$

$$\approx R(t)-\Gamma_2N_2(t)-\pi_\lambda[1+P_\lambda(t)]N_2(t), \quad (2.5b)$$

where

$$N_2(t)=\textstyle\sum_{np}nP(n,p;t), \quad (2.6a)$$

$$P_\lambda(t)=\textstyle\sum_{np}pP(n,p;t). \quad (2.6b)$$

Multiplying (2.4) by p, one can similarly reproduce Eq.

[33] M. Lax and R. D. Hempstead (private communication).

(2.1b). The approximation (2.5b) is justified in these cases because $\pi_\lambda \ll \Gamma_2$.

In the steady-state limit $t \to \infty$ the function $P(n,p;t)$ approaches a fixed limiting form $P(n,p)$ independent of initial conditions. Using that limiting form in Eqs. (2.6) to define $\bar{N}_2$ and $\bar{P}_\lambda$ and making an approximation similar to that of Eq. (2.5b), we can easily verify the steady-state relations (2.2).

The importance of Eq. (2.4) is not that it is equivalent in the manner we have indicated to Eqs. (2.1)–(2.3) but rather that it can be used to specify the *initial conditions* to be utilized with those equations. If in Eq. (1.5) the intensity $I_j(t)$ incident on the photomultiplier j, $j=1$ or 2, is proportional to the radiation intensity in the laser mode λ, it follows from the general theory of optical measurement[12–15] that the intensity correlation function $C_I(\tau)$ is proportional to[34]

$$C_{\lambda\lambda}(\tau)=\langle b_\lambda^\dagger(t)b_\lambda^\dagger(t+|\tau|)b_\lambda(t+|\tau|)b_\lambda(t)\rangle \quad (2.7a)$$

and the function $\Delta C_I(\tau)$ of Eq. (1.10) to

$$\Delta C_{\lambda\lambda}(\tau)=C_{\lambda\lambda}(\tau)-(\langle b_\lambda^\dagger b_\lambda\rangle)^2, \quad (2.7b)$$

where $b_\lambda, b_\lambda^\dagger$ are the photon annihilation and creation operators introduced in Sec. 1 and the expectation value refers to a stationary ensemble of laser systems whose populations are described by the steady-state probability $P(n,p)$.

Given a $\tau \geq 0$, let $P(n,p;t+\tau)_{\lambda,t}$ be the probability that the operator $(b_\lambda^\dagger b_\lambda)(t+\tau)$ in Eq. (2.7) will measure the eigenvalue p and that an atomic level-2 population operator would correspondingly measure the eigenvalue n. This probability is governed in its τ dependence by Eq. (2.4) and has the properties previously ascribed to $P(n,p;t)$. If Φ_{np} is the projection operator for states with eigenvalues (n,p), then

$$P(n,p;t+\tau)_{\lambda,t}=\langle b_\lambda^\dagger(t)\Phi_{np}(t+\tau)b_\lambda(t)\rangle / \sum_{np}\langle b_\lambda^\dagger(t)\Phi_{np}(t+\tau)b_\lambda(t)\rangle = \langle b_\lambda^\dagger(t)\Phi_{np}(t+\tau)b_\lambda(t)\rangle/\bar{P}_\lambda, \quad (2.8)$$

where we have used the completeness property $\sum_{np}\Phi_{np}=1$ and have replaced $\langle b_\lambda^\dagger b_\lambda\rangle$ by $\bar{P}_\lambda$. Taking averages as in Eqs. (2.6), we obtain the functions

$$C_{2\lambda}(\tau)=\bar{P}_\lambda\sum_{np} nP(n,p;t+\tau)_{\lambda,t} = \bar{P}_\lambda N_2(t+\tau)_{\lambda,t}, \quad (2.9a)$$

$$C_{\lambda\lambda}(\tau)=\bar{P}_\lambda\sum_{np} pP(n,p;t+\tau)_{\lambda,t} = \bar{P}_\lambda P_\lambda(t+\tau)_{\lambda,t}. \quad (2.9b)$$

That the function (2.9b) is identical to the function (2.7a) follows from Eq. (2.8). As before, we remove large-τ limiting values to obtain

$$\Delta C_{2\lambda}(\tau)=C_{2\lambda}(\tau)-\bar{P}_\lambda\bar{N}_2, \quad (2.10)$$

[34] Constants of proportionality connecting $C_I(\tau)$ and $C_{\lambda\lambda}(\tau)$ cancel from ratios of the type (1.15) and (1.19b): $C_I(\tau)/C_I(\infty)=C_{\lambda\lambda}(\tau)/C_{\lambda\lambda}(\infty)$, $\Delta P_I(\omega)/C_I(\infty)=\Delta P_{\lambda\lambda}(\omega)/C_{\lambda\lambda}(\infty)$, etc.

etc. Power spectra follow as in Eqs. (1.6) and (1.11) if, consistent with (2.7a), we define $\Delta C_{2\lambda}(-|\tau|)=\Delta C_{2\lambda}(|\tau|)$, etc.

Because the functions $C_{2\lambda}(\tau)$ and $C_{\lambda\lambda}(\tau)$ have been identified in Eqs. (2.9) with populations described by Eqs. (2.1)–(2.3), the functions (2.10) will satisfy in the linear approximation (2.3) the differential equations ($\tau>0$)

$$((\partial/\partial\tau)+\bar{\Gamma}_2)\Delta C_{2\lambda}(\tau)+\pi_\lambda\bar{N}_2\Delta C_{\lambda\lambda}(\tau) = \langle b_\lambda^\dagger(t)r(t+\tau)b_\lambda(t)\rangle, \quad (2.11a)$$

$$-\pi_\lambda(1+\bar{P}_\lambda)\Delta C_{2\lambda}(\tau)+((\partial/\partial\tau)+\bar{\gamma}_\lambda)\Delta C_{\lambda\lambda}(\tau) = \langle b_\lambda^\dagger(t)s(t+\tau)b_\lambda(t)\rangle, \quad (2.11b)$$

in which for notational conciseness we have introduced

$$\bar{\Gamma}_2\equiv\Gamma_2+\pi_\lambda(1+\bar{P}_\lambda), \qquad \bar{\gamma}_\lambda=\gamma_\lambda-\pi_\lambda\bar{N}_2=\gamma_\lambda/(1+\bar{P}_\lambda). \quad (2.12)$$

Assuming that the noise sources $r(t)$, $s(t)$ on the right-hand side of Eqs. (2.11) represent only bona-fide external noise signals, we must supplement Eqs. (2.11) by the *quantum* initial conditions

$$\Delta C_{2\lambda}(0)_Q=Q_{2\lambda}, \quad \Delta C_{\lambda\lambda}(0)_Q=Q_{\lambda\lambda}, \quad (2.13)$$

where from the definitions (2.8) and (2.9)

$$Q_{\lambda\lambda}=\sum_{np}p(p-1)P(n,p)-\bar{P}_\lambda^2, \quad (2.14a)$$

$$Q_{2\lambda}=\sum_{np}npP(n,p)-\bar{N}_2\bar{P}_\lambda. \quad (2.14b)$$

The subscript Q in Eqs. (2.13) indicates that the given initial values relate only to intrinsic quantum fluctuations and that additional contributions to $\Delta C_{\lambda\lambda}(0)$, etc., can result from the noise sources $r(t)$, $s(t)$.

Because Eqs. (2.11) are linear, we can write their solution as the sum of that solution of the homogeneous $[r(t), s(t)=0]$ equations which satisfies the quantum boundary conditions (2.13) and that particular solution of the inhomogeneous $[r(t), s(t)\neq 0]$ equations which vanishes when $r(t)=s(t)=0$. Consider the inhomogeneous equations first. Assume that $r(t)$ and $s(t)$ are real stationary classical variables with power spectra $\Delta P_{RR}(\omega)$, $\Delta P_{RS}(\omega)=\Delta P_{SR}(-\omega)$, and $\Delta P_{SS}(\omega)$, where typically

$$\Delta P_{RS}(\omega)=\int_{-\infty}^{\infty}d\tau\, e^{i\omega\tau}\langle r(t+\tau)s(t)\rangle_t. \quad (2.15)$$

In much the same way that Eq. (1.8) follows from Eqs. (1.3) and (1.7), it follows from Eqs. (2.11) that the component $\Delta P_{\lambda\lambda}(\omega)_{RS}$ of the power spectrum $\Delta P_{\lambda\lambda}(\omega)$ of $\Delta C_{\lambda\lambda}(\tau)$ which derives from the pump fluctuations $r(t)$ and the noise signals $s(t)$ is

$$\Delta P_{\lambda\lambda}(\omega)_{RS}=\{\pi_\lambda^2(1+\bar{P}_\lambda)^2\Delta P_{RR}(\omega)+\pi_\lambda(1+\bar{P}_\lambda) \times[(i\omega+\bar{\Gamma}_2)\Delta P_{RS}(\omega)+(-i\omega+\bar{\Gamma}_2)\Delta P_{SR}(\omega)] +(\omega^2+\bar{\Gamma}_2^2)\Delta P_{SS}(\omega)\}/\{(\bar{\gamma}_\lambda\bar{\Gamma}_2+\pi_\lambda\gamma_\lambda\bar{P}_\lambda-\omega^2)^2 +\omega^2(\bar{\Gamma}_2+\bar{\gamma}_\lambda)^2\}. \quad (2.16)$$

It remains to compute that component $\Delta P_{\lambda\lambda}(\omega)_Q$ of the power spectrum which describes the intrinsic quantum noise. Solving the homogeneous $[r(t), s(t)=0]$ equations (2.11) subject to the initial conditions (2.13), we find

$$\Delta P_{\lambda\lambda}(\omega)_Q=2\{[\pi_\lambda(1+\bar{P}_\lambda)Q_{2\lambda}+\bar{\Gamma}_2Q_{\lambda\lambda}] \times(\bar{\gamma}_\lambda\bar{\Gamma}_2+\pi_\lambda\gamma_\lambda\bar{P}_\lambda-\omega^2)+\omega^2(\bar{\Gamma}_2+\bar{\gamma}_\lambda)Q_{\lambda\lambda}\}/ \{(\bar{\gamma}_\lambda\bar{\Gamma}_2+\pi_\lambda\gamma_\lambda\bar{P}_\lambda-\omega^2)^2+\omega^2(\bar{\Gamma}_2+\bar{\gamma}_\lambda)^2\}. \quad (2.17)$$

Summing the components (2.16) and (2.17), we obtain the total power spectrum of the function (2.7b)

$$\Delta P_{\lambda\lambda}(\omega)=\{\pi_\lambda^2(1+\bar{P}_\lambda)^2[\Delta P_{RR}(\omega)+\Delta_{RR}]+\pi_\lambda(1+\bar{P}_\lambda) \times[(i\omega+\bar{\Gamma}_2)[\Delta P_{RS}(\omega)+\Delta_{RS}]+(-i\omega+\bar{\Gamma}_2) \times[\Delta P_{RS}(\omega)+\Delta_{RS}]]+(\omega^2+\bar{\Gamma}_2^2)[\Delta P_{SS}(\omega)+\Delta_{SS}]\}/ \{(\bar{\gamma}_\lambda\bar{\Gamma}_2+\pi_\lambda\gamma_\lambda\bar{P}_\lambda-\omega^2)^2+\omega^2(\bar{\Gamma}_2+\bar{\gamma}_\lambda)^2\}. \quad (2.18)$$

In this equation we have eliminated the initial values (2.4) in favor of new real parameters

$$\Delta_{RR}=2[\bar{\Gamma}_2Q_{22}+\bar{\gamma}_\lambda\bar{P}_\lambda Q_{2\lambda}],$$
$$\Delta_{RS}=\Delta_{SR}=\bar{\gamma}_\lambda\bar{P}_\lambda Q_{\lambda\lambda}+(\bar{\Gamma}_2+\bar{\gamma}_\lambda)Q_{2\lambda} -\pi_\lambda(1+\bar{P}_\lambda)Q_{22}, \quad (2.19)$$
$$\Delta_{SS}=2[\bar{\gamma}_\lambda Q_{\lambda\lambda}-\pi_\lambda(1+\bar{P}_\lambda)Q_{2\lambda}],$$

which are undetermined to within an unspecified constant Q_{22}. It will prove useful below and in Sec. 3 to arbitrarily fix Q_{22} by the moment relation

$$Q_{22}=\sum_{np} n(n-1)P(n,p)-\bar{N}_2^2 \quad (2.20)$$

analogous to the definitions (2.14).

To evaluate the parameters (2.19), we use the STT method. Setting $R(t)=\bar{R}$ in Eq. (2.4), passing to the steady-state limit $[t\to\infty, P(n,p;t)\to P(n,p)]$, and successively computing the second-order moments of Eqs. (2.14) and (2.20), we obtain the three equations

$$\bar{\gamma}_\lambda\bar{P}_\lambda^2=-\pi_\lambda(1+\bar{P}_\lambda)Q_{2\lambda}+\bar{\gamma}_\lambda Q_{\lambda\lambda},$$
$$\bar{\gamma}_\lambda\bar{P}_\lambda^2=\pi_\lambda(1+\bar{P}_\lambda)Q_{22}-(\bar{\Gamma}_2+\bar{\gamma}_\lambda)Q_{2\lambda}-\bar{\gamma}_\lambda\bar{P}_\lambda Q_{\lambda\lambda}, \quad (2.21)$$
$$0=\bar{\Gamma}_2Q_{22}+\bar{\gamma}_\lambda\bar{P}_\lambda Q_{2\lambda}.$$

Comparing Eqs. (2.19) and (2.21), we see immediately that

$$\Delta_{RR}=0, \quad \Delta_{RS}=\Delta_{SR}=-\bar{\gamma}_\lambda\bar{P}_\lambda^2, \quad \Delta_{SS}=2\bar{\gamma}_\lambda\bar{P}_\lambda^2. \quad (2.22)$$

Substituting these results into (2.18), we obtain for the quantum-fluctuation component (2.17) of the power spectrum

$$\Delta P_{\lambda\lambda}(\omega)_Q=2\bar{\gamma}_\lambda\bar{P}_\lambda^2(\omega^2+\Gamma_2\bar{\Gamma}_2)/ \{(\bar{\gamma}_\lambda\bar{\Gamma}_2+\pi_\lambda\gamma_\lambda\bar{P}_\lambda-\omega^2)^2+\omega^2(\bar{\Gamma}_2+\bar{\gamma}_\lambda)^2\}. \quad (2.23)$$

Actually solving Eqs. (2.21) for $Q_{\lambda\lambda}$, which is feasible for this simple example, we obtain the total integrated quantum-fluctuation power spectrum

$$\Delta C_{\lambda\lambda}(0)_Q=\frac{\bar{\gamma}_\lambda\bar{P}_\lambda^2(\Gamma_2\bar{\Gamma}_2+\bar{\gamma}_\lambda\bar{\Gamma}_2+\pi_\lambda\gamma_\lambda\bar{P}_\lambda)}{(\bar{\Gamma}_2+\bar{\gamma}_\lambda)(\bar{\gamma}_\lambda\bar{\Gamma}_2+\pi_\lambda\gamma_\lambda\bar{P}_\lambda)}. \quad (2.24)$$

For weak pumping, well below threshold, $\pi_\lambda\gamma_\lambda\bar{P}_\lambda \ll\bar{\gamma}_\lambda\bar{\Gamma}_2=\pi_\lambda\gamma_\lambda+\gamma_\lambda\bar{\Gamma}_2/(1+\bar{P}_\lambda)$. If the noise signals $r(t)$ and $s(t)$ are statistically independent $[\Delta P_{RS}(\omega)=0]$,[35] then

$$\Delta P_{\lambda\lambda}(\omega)\Big|_{\substack{\text{weak}\\\text{pump}}}=\frac{\pi_\lambda^2(1+\bar{P}_\lambda)^2\Delta P_{RR}(\omega)}{(\omega^2+\bar{\gamma}_\lambda^2)(\omega^2+\bar{\Gamma}_2^2)} +\frac{\Delta P_{SS}(\omega)+2\bar{\gamma}_\lambda\bar{P}_\lambda^2}{\omega^2+\bar{\gamma}_\lambda^2}. \quad (2.25a)$$

The total integrated intensity (2.24) of the quantum fluctuations is

$$\Delta C_{\lambda\lambda}(0)_Q\Big|_{\substack{\text{weak}\\\text{pump}}}=\bar{P}_\lambda^2. \quad (2.25b)$$

There is no amplitude stabilization. Noise amplitude modulation and noise phase modulation contribute comparably to the observed spectral linewidth of the laser output. The intrinsic intensity fluctuations are those expected from a thermal-equilibrium photon field having an exponential distribution (Bose-Einstein-Planck distribution) with an average number $\bar{P}_\lambda$ of photons.[36] If $\nu_0=\omega_0/2\pi$ is the photon frequency, the noise temperature is

$$T\Big|_{\substack{\text{weak}\\\text{pump}}}=\hbar\omega_0/k\,\ln[(1+\bar{P}_\lambda)/\bar{P}_\lambda]\xrightarrow[\bar{P}_\lambda>>1]{}\hbar\omega_0\bar{P}_\lambda/k. \quad (2.26)$$

For strong pumping, well above threshold, $\bar{P}_\lambda\gg1$ and $\pi_\lambda\gamma_\lambda\bar{P}_\lambda\gg\bar{\gamma}_\lambda\bar{\Gamma}_2$. In this case, if $r(t)$ and $s(t)$ are statistically independent,[35]

$$\Delta P_{\lambda\lambda}(\omega)\Big|_{\substack{\text{strong}\\\text{pump}}}=\frac{(\pi_\lambda\bar{P}_\lambda)^2\Delta P_{RR}(\omega)+(\omega^2+\bar{\Gamma}_2^2)\Delta P_{SS}(\omega)+2(\omega^2+\Gamma_2\bar{\Gamma}_2)\gamma_\lambda\bar{P}_\lambda}{(\pi_\lambda\gamma_\lambda\bar{P}_\lambda-\omega^2)^2+\omega^2(\bar{\Gamma}_2+\bar{\gamma}_\lambda)^2} \quad (2.27a)$$

and

$$\Delta C_{\lambda\lambda}(0)_Q\Big|_{\substack{\text{strong}\\\text{pump}}}=\frac{\Gamma_2\bar{\Gamma}_2+\pi_\lambda\gamma_\lambda\bar{P}_\lambda}{\pi_\lambda(\bar{\Gamma}_2+\bar{\gamma}_\lambda)}\xrightarrow[\bar{P}_\lambda\to\infty]{}\frac{\Gamma_2+\gamma_\lambda}{\pi_\lambda}. \quad (2.27b)$$

[35] Generalizations appropriate to $\Delta P_{RS}(\omega)\neq0$, etc., can easily be derived from $\Delta P_{\lambda\lambda}(\omega)_{RS}$ equations like (2.16).

[36] R. J. Glauber, Phys. Rev. Letters **10**, 84 (1963), and Phys. Rev. **131**, 2766 (1963); E. Wolf and C. L. Mehta, Phys. Rev. Letters **13**, 705 (1964). [L. Mandel and E. Wolf, Phys. Rev. **124**, 1696 (1961), assume a Gaussian electromagnetic field distribution to describe the output from lasers. This is consistent with our weak-pump results (2.25) and (2.26) but not with our strong-pump results. (Compare Ref. 28.)]

Here there is appreciable amplitude stabilization. Quantum-noise amplitude modulation contributes insignificantly to the spectral linewidth of the output. The intrinsic intensity fluctuations (2.27b) are, to within the $\bar{P}_\lambda$-independent constant $(\Gamma_2+\gamma_\lambda)/\pi_\lambda$, those which would be expected from a classical field having a Poisson distribution (Maxwell-Boltzmann distribution).[36]

At low frequencies the stabilized spectral function (2.23) is less than the unstabilized function (2.25a) evaluated for the same value of $\bar{P}_\lambda$. At very high frequencies both functions approximate

$$\Delta P_{\lambda\lambda}(\omega)\,|_{\text{high freq.}}=\{\pi_\lambda^2(1+\bar{P}_\lambda)^2\Delta P_{RR}(\omega)+\omega^2[\Delta P_{SS}(\omega)+2\bar{\gamma}_\lambda\bar{P}_\lambda^2]\}/\omega^4. \quad (2.28)$$

In this high-frequency limit amplitude stabilization is ineffective because the population inversion with its own finite response time is unable to follow and (thereby stabilize) the fluctuations of the photon field. At intermediate frequencies the function (2.23) does in some cases exceed the unstabilized function (2.25a). This is a resonance phenomenon and will be considered in more detail in Sec. 6.

3. LANGEVIN TREATMENT OF QUANTUM FLUCTUATIONS

In the preceding section we used the STT method[30] to compute the intrinsic quantum population fluctuations of a simple four-level laser. While the STT method clearly demonstrates the physical origin of the quantum noise, it is cumbersome and not well suited to the analysis of more complicated laser systems. For the prototype system of Sec. 2 it is feasible to actually solve Eqs. (2.21) for the initial-condition parameters $Q_{\lambda\lambda}$, etc., and to use the results to complete Eq. (2.17); however, the algebraic complications in this approach are so severe in more general systems that it is important to develop a simpler but physically equivalent alternative to the STT method. Because the differential equations (2.11) can be directly inferred from the linearized rate-equations (2.3) without using Eq. (2.4), the essential problem is to incorporate the STT boundary conditions.

By introducing constants (2.19) which add to the noise spectra (2.15), we can always incorporate the quantum-fluctuation power spectrum (2.17) into the noise-signal spectrum (2.16). This suggests that we interpret the intrinsic quantum fluctuations of systems described by rate-equations in terms of fictitious Langevin noise sources $r(t)$,$s(t)$ whose spectra (2.14) are the frequency-independent constants (2.19).

Shot noise associated with δ-function impulses arriving (or departing) at a prescribed average rate has a frequency-independent or *white-noise* power spectrum. If the impulses in a signal $r(t)$ have constant integrated intensity α and if their average rates of arrival $(+\alpha)$ and departure $(-\alpha)$ are respectively R_+ and R_-, then the average value of $r(t)$ is[27]

$$\langle r(t)\rangle_t=\alpha(R_+-R_-), \quad (3.1a)$$

and the power spectrum of the autocorrelation function (2.15) is[27]

$$\Delta P_{RR}(\omega)=\int_{-\infty}^{\infty}d\tau\, e^{i\omega\tau}\langle[r(t+\tau)-\bar{r}][r(t)-\bar{r}]\rangle_t$$
$$=(+\alpha)^2R_++(-\alpha)^2R_-=\alpha^2(R_++R_-). \quad (3.1b)$$

The cross-correlation function of two different signals has a similar form,

$$\Delta P_{R_1R_2}(\omega)=\alpha^2[(R_++R_-)_+-(R_++R_-)_-], \quad (3.2)$$

except that the rates describe impulses which occur simultaneously in both signals, $(R_++R_-)_+$ being the rate of impulses which have the same sign in both signals and $(R_++R_-)_-$ being that of impulses with different signs.

In Eq. (2.4) both the photon quantum number p and the level-2 population quantum number n change by unit increments. This suggests that a shot-noise Langevin model in which the quantum-noise components of $r(t)$ and $s(t)$ are δ-function impulses of unit-integrated intensity might reproduce the STT results. This would indeed be the case if the correlation functions (2.9) had been based upon the joint probability $P(n,p;n',p';t+\tau,t)$ that the quantum numbers (n,p) obtain at time $t+\tau$ if (n',p') obtain at time t. The correlation function analogous to that of (2.7a) would then have been

$$C_{\lambda\lambda'}(\tau)=\langle(b_\lambda^\dagger b_\lambda)(t+\tau)(b_\lambda^\dagger b_\lambda)(t)\rangle \quad (3.3a)$$
$$=\sum_{np}\sum_{n'p'}pp'P(n,p;n',p';t+\tau,t). \quad (3.3b)$$

Because Eq. (2.4) also applies here, the function (3.3) satisfies differential equations analogous to Eqs. (2.11). However, the initial conditions

$$Q_{\lambda\lambda'}=\sum_{np}p^2P(n,p)-\bar{P}_\lambda^2=Q_{\lambda\lambda}+\bar{P}_\lambda, \quad (3.4a)$$
$$Q_{2\lambda'}=\sum_{np}npP(n,p)-\bar{N}_2\bar{P}_\lambda=Q_{2\lambda}, \quad (3.4b)$$
$$Q_{22'}=\sum_{np}n^2P(n,p)-\bar{N}_2^2=Q_{22}+\bar{N}_2, \quad (3.4c)$$

differ from those of Eqs. (2.14) and (2.20). Using these new initial conditions in Eqs. (2.19), we would find the new noise sources

$$\Delta_{RR'}=\Delta_{RR}+2\bar{\Gamma}_2N_2=\bar{R}+\Gamma_2\bar{N}_2+\pi_\lambda(1+\bar{P}_\lambda)\bar{N}_2, \quad (3.5a)$$
$$\Delta_{RS'}=\Delta_{SR'}=\Delta_{RS}-\bar{\gamma}_\lambda\bar{P}_\lambda=-\pi_\lambda(1+\bar{P}_\lambda)\bar{N}_2, \quad (3.5b)$$
$$\Delta_{SS'}=\Delta_{SS}+2\bar{\gamma}_\lambda\bar{P}=\pi_\lambda(1+\bar{P}_\lambda)\bar{N}_2+\gamma_\lambda\bar{P}_\lambda. \quad (3.5c)$$

These are precisely the noise sources which would be predicted from Eqs. (2.1), (3.1), and (3.2) in a Langevin model which associates a noise impulse of unit-integrated intensity with each change in atomic or photon population.

One might object to "noise" in the above model being associated with the transfer of excitation between the atoms and the photon field, since that transfer is presumably described by an atom-photon interaction Hamiltonian which does not directly involve dissipation or external reservoirs. In Paper III it will be shown that this transfer noise is an indirect consequence of the reservoir interaction responsible for the finite linewidth of the atomic transition and that the noise has a bandwidth comparable to that linewidth. A white-noise spectrum results from the rate equations because in deriving those equations one must assume that the atomic linewidth is large compared with fluctuation frequencies.

The two principal advantages of the shot-noise model are that it provides a simple physical explanation of the origin of the intrinsic quantum fluctuations and that it permits one to infer the magnitude of the quantum-noise sources from an inspection of the *form* of the dynamic equations (3.1), without directly using Eq. (2.4). This simple classical model is applicable to the function (3.3) principally because only commuting population operators enter its rate-equation analysis.[37] Because the parameters (2.22) violate the Schwarz inequality applicable to classical noise sources,

$$|\Delta P_{RS}(\omega)| \leq [\Delta P_{RR}(0)\Delta P_{SS}(0)]^{1/2}, \tag{3.6}$$

it is clear that a Langevin model with classical noise sources is not always applicable—in particular, it is not directly applicable to the rate-equation analysis of the functions (2.7). Lax has shown[38] that the Langevin noise sources appropriate to quantum systems are *operators* whose commutation properties cannot be neglected. These commutation properties are responsible for the differences noted in Eqs. (3.5) between the spectral parameters (2.19) and those predicted by the shot-noise model applicable to the function (3.3).

Although the shot-noise model is not immediately applicable to the experimental functions (2.7) because of their special operator ordering, it nevertheless does provide some insight into the origin of the quantum fluctuations, and it can be used to compute the relevant noise parameters if one independently computes the commutator-induced differences $\delta\Delta_{RR}=\Delta_{RR}-\Delta_{RR}'$, etc. The following general remarks are relevant to the latter calculation. Let $Z_m(t)$ be a set of atomic and photon populations described by rate-equations of the type (2.1), let $z_m(t)=Z_m(t)-\bar{Z}_m$ represent a small fluctuation of $Z_m(t)$ about its mean $\bar{Z}_m$, and let the $z_m(t)$ satisfy a set of linear equations like (2.3)

$$(\partial/\partial t)z_m(t)=\sum_n \Lambda_{mn}z_n(t), \tag{3.7}$$

where $\mathbf{\Lambda}$ is a coefficient matrix. In this notation the Einstein relations (2.19) take the form[37,38]

$$\Delta_{mn}=-\sum_l\{\Lambda_{ml}Q_{ln}+Q_{ml}(\Lambda^\dagger)_{ln}\}. \tag{3.8}$$

If Q_{mm} is defined as in Eqs. (2.14) and (2.20) and Q_{mn}' as in Eqs. (3.4), then

$$\delta Q_{mn}=Q_{mn}-Q_{mn}'=-\delta_{mn}\bar{Z}_n \tag{3.9}$$

and

$$\begin{aligned}\delta\Delta_{mn}&=\Delta_{mn}-\Delta_{mn}'=-\sum_l\{\Lambda_{ml}\delta Q_{ln}+\delta Q_{ml}(\Lambda^\dagger)_{ln}\}\\&=\Lambda_{mn}\bar{Z}_n+\bar{Z}_m(\Lambda^\dagger)_{mn}=\delta\Delta_{nm}{}^*.\end{aligned} \tag{3.10a}$$

If $\mathbf{\Lambda}$ is real

$$\delta\Delta_{mn}=\Lambda_{mn}\bar{Z}_n+\Lambda_{nm}\bar{Z}_m=\delta\Delta_{nm}. \tag{3.10b}$$

This result, when combined with the shot-noise prescription for the calculation of the parameters Δ_{mn}', permits us to infer the magnitude of the noise parameters (2.19) from an inspection of the *form* of the dynamic equations without the intermediate use of the probability equation (2.4).

It is important to realize that the noise parameters computed by the above prescription are not simply reasonable approximations to noise sources present in lasers but are *the* noise sources prescribed by the initial conditions intrinsic to the dynamic model. The fundamental and intimate general connection between the operator Langevin noise sources of a quantum mechanical system and the operator equations of motion in that system has been strongly emphasized by Lax.[38]

A shot-noise model of laser quantum noise similar to that outlined in Eqs. (3.3)–(3.5) has been used by Haken.[39]

4. FOUR-LEVEL LASER, SEVERAL PHOTON MODES

Using the Langevin model of quantum fluctuations outlined in Sec. 3, we can readily generalize the results of Sec. 2 to determine the intensity fluctuations of several modes excited by the same atomic transition. In the same sense that $N_j(t)$ and $P_\lambda(t)$ in Eqs. (2.1) are the average values of atomic and photon population operators with respect to some initial-value ensemble, we define $D_{\lambda\nu}(t)$ to be the average value of the photon operator $(b_\nu{}^\dagger b_\lambda)(t)$ and $N_j{}^M(t)$ to be the average value of the level-j population operator of atom M, $M=1$ to N_T. The photon population $P_\lambda(t)=D_{\lambda\lambda}(t)$, and the atomic population $N_j(t)=\sum_M N_j{}^M(t)$. For each photon mode λ we introduce coefficients $u_\lambda{}^M$ such that the average photon intensity at atom M is

$$D^M(t)=\sum_{\lambda\nu}(u_\lambda{}^M)^*D_{\lambda\nu}(t)u_\nu{}^M, \tag{4.1}$$

[37] For a more general discussion of noise in classical systems cf. M. Lax, Rev. Mod. Phys. 32, 25 (1960), especially Sec. 5, where the connection between Markoff and Langevin methods is considered.

[38] M. Lax (to be published). These results will play a central role in Paper III of the present series. Cf. also M. Lax, in *Proceedings of the Physics of Quantum Electronics Conference, San Juan, Puerto Rico, 1965*, edited by P. L. Kelley, B. Lax, and P. E. Tannenwald (McGraw-Hill Book Company, Inc., New York, 1965).

[39] H. Haken, Z. Physik 181, 96 (1964); 182, 346 (1965).

where the sum is over the several photon modes relevant to the calculation. We also define

$$N_{j,\lambda\nu}(t)=\sum_M (u_\nu{}^M)^* N_j{}^M(t) u_\lambda{}^M. \quad (4.2)$$

If we assume that the lower laser-level population is negligible [$N_1(t)=0$, as before], that there is no mode locking, and that the atomic linewidth is large compared with both the fluctuation frequencies and the mode difference frequencies $\omega_{\lambda\nu}=\omega_\lambda-\omega_\nu$, the rate-equations (2.1) can be generalized as follows[40]:

$$(\partial/\partial t)N_2{}^M(t)=R^M(t)-\Gamma_2 N_2{}^M(t) -\pi_0 N_2{}^M(t)\sum_{\rho\sigma}(u_\rho{}^M)^* \times[\delta_{\rho\sigma}+D_{\rho\sigma}(t)]u_\sigma{}^M, \quad (4.3a)$$

$$(\partial/\partial t)D_{\lambda\nu}(t)=s_{\lambda\nu}(t)-[\tfrac{1}{2}(\gamma_\lambda+\gamma_\nu)+i\omega_{\lambda\nu}]D_{\lambda\nu}(t) +\tfrac{1}{2}\pi_0\sum_\rho\{N_{2,\lambda\rho}(t)[\delta_{\rho\nu}+D_{\rho\nu}(t)] +[\delta_{\lambda\rho}+D_{\lambda\rho}(t)]N_{2,\rho\nu}(t)\}, \quad (4.3b)$$

where π_0 is a non-negative coupling constant. If the atoms fill the laser cavity uniformly, as we assume, then, because the different photon modes are orthogonal,

$$\pi_0\sum_M (u_\lambda{}^M)^* u_\nu{}^M=\pi_\lambda N_T\delta_{\lambda\nu}, \quad (4.4)$$

where π_λ is a non-negative constant. In the steady state we assume that the time-averaged fields seen by each atom are identical. This implies with Eqs. (4.3) and (4.4) that

$$\bar{N}_2{}^M=N_2/N_T, \quad \bar{N}_{2,\lambda\nu}=(\pi_\lambda\bar{N}_2/\pi_0)\delta_{\lambda\nu}, \quad (4.5a)$$

$$\bar{D}_{\lambda\nu}=\bar{P}_\lambda\delta_{\lambda\nu}, \quad \bar{D}^M=\sum_\lambda \pi_\lambda(1+\bar{P}_\lambda)/\pi_0, \quad (4.5b)$$

where [compare Eqs. (2.2)]

$$\bar{R}=\Gamma_2\bar{N}_2+\sum_\lambda \pi_\lambda(1+\bar{P}_\lambda)\bar{N}_2, \quad (4.6a)$$

$$\gamma_\lambda\bar{P}_\lambda=\pi_\lambda(1+\bar{P}_\lambda)\bar{N}_2. \quad (4.6b)$$

If $d_{\lambda\nu}(t)=D_{\lambda\nu}(t)-\bar{D}_{\lambda\nu}$, etc., are small fluctuations of the variables in Eqs. (4.3) about their time-averaged values, then to first order in these fluctuations [compare Eqs. (2.3)]

$$(\partial/\partial t)n_{2,\lambda\nu}(t)=r_{\lambda\nu}(t)-\bar{\Gamma}_2 n_{2,\lambda\nu}(t) -\pi_0\bar{N}_2\sum_{\rho\sigma}C(\lambda\sigma;\nu\rho)d_{\rho\sigma}(t) \approx r_{\lambda\nu}(t)-\bar{\Gamma}_2 n_{2,\lambda\nu}(t)-(\pi_\lambda\pi_\nu/\pi_0)\bar{N}_2 d_{\lambda\nu}(t) -\delta_{\lambda\nu}\pi_\lambda\bar{N}_2\sum_{\rho\neq\lambda}{}'\,\pi_\rho d_{\rho\rho}(t)/\pi_0, \quad (4.7a)$$

$$d_{\lambda\nu}(t)=s_{\lambda\nu}(t)-[\tfrac{1}{2}(\bar{\gamma}_\lambda+\bar{\gamma}_\nu)+i\omega_{\lambda\nu}]d_{\lambda\nu}(t) +\tfrac{1}{2}\pi_0[(1+\bar{P}_\lambda)+(1+\bar{P}_\nu)]n_{2,\lambda\nu}(t), \quad (4.7b)$$

where [compare Eqs. (2.12)]

$$\bar{\Gamma}_2=\Gamma_2+\sum_\lambda \pi_\lambda(1+\bar{P}_\lambda), \quad (4.8a)$$

$$\bar{\gamma}_\lambda=\gamma_\lambda-\pi_\lambda\bar{N}_2=\gamma_\lambda/(1+\bar{P}_\lambda), \quad (4.8b)$$

and

$$C(\lambda\sigma;\nu\rho)=(1/N_T)\sum_M u_\lambda{}^M u_\sigma{}^M(u_\nu{}^M u_\rho{}^M)^*. \quad (4.9)$$

The approximation to this last function which we have used in (4.7a) is reasonable when Eqs. (4.4) and (4.5) obtain.

The first-order equations (4.7) effect a separation between diagonal ($\lambda=\nu$) and off-diagonal ($\lambda\neq\nu$) elements of the averages $D_{\lambda\nu}(t)$ and $N_{2,\lambda\nu}(t)$. This separation has the physical implication that population pulsations driven by the beating fields from different modes will not be observable in the photon intensities $P_\lambda(t)=D_{\lambda\lambda}(t)$. Beats will be seen by detectors which measure the off-diagonal elements $D_{\lambda\nu}(t)$, $\lambda\neq\nu$, and population pulsations will be seen by those which detect the emission from separate atoms or small groups of atoms—that is, by detectors which measure the atomic population $N_2{}^M(t)$.[41] An experimental measure of the accuracy of the first-order theory of this section is the extent to which the diagonal elements $D_{\lambda\lambda}(t)$ are free from beat-frequency pulsations.

In multimode lasers the intensity correlation experiments described in the introduction measure the correlation functions[12–15]

$$C_{(\lambda\lambda')(\nu\nu')}(\tau)=\langle\bar{T}\{b_{\nu'}{}^\dagger(t)b_{\lambda'}{}^\dagger(t+\tau)b_\lambda(t+\tau)b_\nu(t)\}\rangle \quad (4.10a)$$

and

$$\Delta C_{(\lambda\lambda')(\nu\nu')}(\tau)=C_{(\lambda\lambda')(\nu\nu')}(\tau) -\langle(b_{\lambda'}{}^\dagger b_\lambda)(t+\tau)\rangle\langle(b_{\nu'}{}^\dagger b_\nu)(t)\rangle, \quad (4.10b)$$

where $\bar{T}$ indicates time ordering such that the operator ordering in (4.10a) remains as indicated for $\tau>0$ and such that the $b^\dagger$ operators are interchanged and the b operators are interchanged if $\tau<0$. Because the ensemble implicit in the expectation value is assumed stationary, it follows that

$$C_{(\lambda\lambda')(\nu\nu')}(-|\tau|)=C_{(\nu\nu')(\lambda\lambda')}(|\tau|). \quad (4.11)$$

The functions (4.10) reduce to the functions (2.7) for single-mode systems. When Eqs. (4.7) obtain, the functions (4.10) are different from zero only when ($\lambda=\lambda'$, $\nu=\nu'$) or ($\lambda=\nu'$, $\nu=\lambda'$). Corresponding to these two cases, we introduce new functions

$$C_{\lambda\nu}(\tau)=\langle\bar{T}\{b_\nu{}^\dagger(t)b_\lambda{}^\dagger(t+\tau)b_\lambda(t+\tau)b_\nu(t)\}\rangle, \quad (4.12a)$$

$$\Delta C_{\lambda\nu}(\tau)=C_{\lambda\nu}(\tau)-\bar{P}_\lambda\bar{P}_\nu, \quad (4.12b)$$

[40] Cf. Paper III; also, M. Lax (to be published). The assumption of no mode locking enters when we use a product of averages—for example, $N_2{}^M(t)D_{\rho\sigma}(t)$ in Eq. (4.3a)—in place of a single average of operator products. Although a similar approximation was justified in the single-mode Eqs. (2.5) simply because $\pi_\lambda\ll\Gamma_2$, the multimode case is complicated by beat-frequency resonances which enhance the importance of photon-atom correlations. (Cf. Ref. 3.)

[41] The photon modes λ enumerated in the equations of Sec. 4 are not a complete set of modes for the radiation field but are only the low-loss modes relevant to laser oscillation. [Cf. A. G. Fox and T. Li, Bell System Tech. J. **40**, 61 (1961)]. It is to the latter modes that Eq. (4.4) and the concomitant separation of Eqs. (4.7) into diagonal and off-diagonal components pertain. Equation (4.4) does not pertain, for example, to spontaneous emission perpendicular to the axis of a gas laser.

and

$$C_{\lambda\nu}'(\tau)=\langle \bar{T}\{b_\lambda^\dagger(t)b_\nu^\dagger(t+\tau)b_\lambda(t+\tau)b_\nu(t)\}\rangle \quad (4.13a)$$

$$=\Delta C_{\lambda\nu}'(\tau). \quad (4.13b)$$

The functions (2.7) are the functions (4.12) with $\lambda=\nu$. [The functions (4.13) are not to be confused with the functions (3.3) used in Sec. 3.]

The functions (4.12) and their linearized equations of motion (4.7) involve only diagonal elements of the photon density matrix; the functions (4.13) involve off-diagonal elements. Because it is not our intention to discuss phase fluctuations in this series of papers and because the functions (4.13) are not relevant to the calculation of the functions (4.12) with Eqs. (4.7), we shall be content with the following approximation to the functions (4.13):

$$C_{\lambda\nu}'(\tau)\approx\langle b_\lambda^\dagger(t)b_\lambda(t+\tau)\rangle\langle b_\nu^\dagger(t+\tau)b_\nu(t)\rangle. \quad (4.14)$$

This approximation is exact in the two extreme cases that the photon fields have second-order coherence[10] or that they have the coherence properties of blackbody radiation. In this approximation the power spectrum

$$\Delta P_{\lambda\nu}'(\omega)=\int_{-\infty}^{\infty}d\tau\, e^{i\omega\tau}\Delta C_{\lambda\nu}'(\tau)$$

$$=\int_{-\infty}^{\infty}\frac{d\bar{\omega}}{2\pi}g_\lambda(\omega+\bar{\omega})g_\nu(\bar{\omega}), \quad (4.15)$$

where

$$g_\lambda(\omega)=\int_{-\infty}^{\infty}d\tau\, e^{i\omega\tau}\langle b_\lambda^\dagger(t)b_\lambda(t+\tau)\rangle. \quad (4.16)$$

The spectrum (4.16) is that which would be measured by familiar dispersion or diffraction spectrometers. The power spectrum $\Delta P_{\lambda\nu}'(\omega)$ is peaked near the difference frequency $\omega_{\lambda\nu}$.

In what follows we concentrate exclusively upon the functions (4.12) whose analysis parallels that of the functions (2.7) in Sec. 2. Making the ansatz $r_{\lambda\lambda}(t)=(\pi_\lambda/\pi_0)r(t)$, defining $s_\lambda(t)=s_{\lambda\lambda}(t)$, and introducing a function $C_{2\lambda}(\tau)$ similar to that in Eq. (2.9a), we obtain from Eqs. (4.7) [compare Eqs. (2.11)]

$$((\partial/\partial\tau)+\bar{\Gamma}_2)\Delta C_{2\nu}(\tau)+\textstyle\sum_\lambda \pi_\lambda\bar{N}_2\Delta C_{\lambda\nu}(\tau)$$

$$=\langle b_\nu^\dagger(t)r(t+\tau)b_\nu(t)\rangle, \quad (4.17a)$$

$$-\pi_\lambda(1+\bar{P}_\lambda)\Delta C_{2\nu}(\tau)+((\partial/\partial\tau)+\bar{\gamma}_\lambda)\Delta C_{\lambda\nu}(\tau)$$

$$=\langle b_\nu^\dagger(t)s_\lambda(t+\tau)b_\nu(t)\rangle. \quad (4.17b)$$

The noise sources $r(t)$ and $s_\lambda(t)$ include fictitious quantum-fluctuation noise sources as well as bona-fide external signals or fluctuations. Using the method of Sec. 3 to compute the quantum-noise spectral parameters, we find [compare Eqs. (2.22)]

$$\Delta_{RR}=0,\quad \Delta_{R\lambda}=\Delta_{\lambda R}=-\bar{\gamma}_\lambda\bar{P}_\lambda^2,\quad \Delta_{\lambda\nu}=2\bar{\gamma}_\lambda\bar{P}_\lambda^2\delta_{\lambda\nu}, \quad (4.18)$$

where in the subscripts we have written λ in place of S_λ.

If $\Delta P_{\lambda\nu}(\omega)$ is the power spectrum of $\Delta C_{\lambda\nu}(\tau)$, let us separate $\Delta P_{\lambda\nu}(\omega)$ as in Sec. 2 into a component $\Delta P_{\lambda\nu}(\omega)_{RS}$ describing bona-fide pump fluctuations and external signals and a component $\Delta P_{\lambda\nu}(\omega)_Q$ describing intrinsic quantum noise. Solving Eqs. (4.17), we write the component $\Delta P_{\lambda\nu}(\omega)_{RS}$ in the form [compare Eq. (2.16)]

$$\Delta P_{\lambda\nu}(\omega)_{RS}=(-i\omega+\bar{\gamma}_\lambda)^{-1}(i\omega+\bar{\gamma}_\nu)^{-1}\left\{\left(\bar{\Gamma}_2+\sum_\mu\frac{\pi_\mu\gamma_\mu\bar{P}_\mu\bar{\gamma}_\mu}{\omega^2+\bar{\gamma}_\mu{}^2}\right)^2+\omega^2\left(1-\sum_\mu\frac{\pi_\mu\gamma_\mu\bar{P}_\mu}{\omega^2+\bar{\gamma}_\mu{}^2}\right)^2\right\}^{-1}$$

$$\times\int_{-\infty}^{\infty}d\tau\, e^{i\omega\tau}\left\{\left[\pi_\lambda(1+\bar{P}_\lambda)r(t+\tau)+\left(-i\omega+\bar{\Gamma}_2+\sum_{\mu\neq\lambda}{}'\frac{\pi_\mu\gamma_\mu\bar{P}_\mu}{-i\omega+\bar{\gamma}_\mu}\right)s_\lambda(t+\tau)-\gamma_\lambda\bar{P}_\lambda\sum_{\mu\neq\lambda}{}'\frac{\pi_\mu}{-i\omega+\bar{\gamma}_\mu}s_\mu(t+\tau)\right]\right.$$

$$\left.\times\left[\pi_\nu(1+\bar{P}_\nu)r(t)+\left(i\omega+\bar{\Gamma}_2+\sum_{\rho\neq\nu}{}'\frac{\pi_\rho\gamma_\rho\bar{P}_\rho}{i\omega+\bar{\gamma}_\rho}\right)s_\nu(t)-\gamma_\nu\bar{P}_\nu\sum_{\rho\neq\nu}{}'\frac{\pi_\rho}{i\omega+\bar{\gamma}_\rho}s_\rho(t)\right]\right\}_{t\text{-averaged}}, \quad (4.19)$$

where we identify the power spectra $\Delta P_{RR}(\omega)$, etc., as in Eq. (2.15). To obtain the power spectrum of the intrinsic quantum noise, we replace the power spectra $\Delta P_{RR}(\omega)$, etc., in (4.19) by the quantum-noise spectral parameters (4.18). Doing that, we obtain the diagonal elements [compare Eq. (2.23)]

$$\Delta P_{\lambda\lambda}(\omega)_Q=(\omega^2+\bar{\gamma}_\lambda{}^2)^{-1}\left\{\left(\bar{\Gamma}_2+\sum_\mu\frac{\pi_\mu\gamma_\mu\bar{P}_\mu\bar{\gamma}_\mu}{\omega^2+\bar{\gamma}_\mu{}^2}\right)^2+\omega^2\left(1-\sum_\mu\frac{\pi_\mu\gamma_\mu\bar{P}_\mu}{\omega^2+\bar{\gamma}_\mu{}^2}\right)^2\right\}^{-1}\left\{2\bar{\gamma}_\lambda\bar{P}_\lambda{}^2\left[\left(\bar{\Gamma}_2+\sum_{\mu\neq\lambda}{}'\frac{\pi_\mu\gamma_\mu\bar{P}_\mu\bar{\gamma}_\mu}{\omega^2+\bar{\gamma}_\mu{}^2}\right)\right.\right.$$

$$\left.\left.\times\left(\bar{\Gamma}_2-\pi_\lambda(1+\bar{P}_\lambda)+\sum_{\mu\neq\lambda}{}'\frac{\pi_\mu\gamma_\mu\bar{P}_\mu\bar{\gamma}_\mu}{\omega^2+\bar{\gamma}_\mu{}^2}\right)+\omega^2\left(1-\sum_{\mu\neq\lambda}{}'\frac{\pi_\mu\gamma_\mu\bar{P}_\mu}{\omega^2+\bar{\gamma}_\mu{}^2}\right)^2\right]+2\gamma_\lambda{}^2\bar{P}_\lambda{}^2\sum_{\mu\neq\lambda}{}'\frac{\pi_\mu{}^2\gamma_\mu\bar{P}_\mu}{\omega^2+\bar{\gamma}_\mu{}^2}\right\} \quad (4.20a)$$

and the off-diagonal elements ($\lambda \neq \nu$)

$$\Delta P_{\lambda\nu}(\omega)_Q = (-i\omega+\bar{\gamma}_\lambda)^{-1}(i\omega+\bar{\gamma}_\nu)^{-1}\left\{\left(\bar{\Gamma}_2+\sum_\mu \frac{\pi_\mu\gamma_\mu\bar{P}_\mu\bar{\gamma}_\mu}{\omega^2+\bar{\gamma}_\mu{}^2}\right)^2+\omega^2\left(1-\sum_\mu \frac{\pi_\mu\gamma_\mu\bar{P}_\mu}{\omega^2+\bar{\gamma}_\mu{}^2}\right)^2\right\}^{-1}$$

$$\times\left\{-\bar{\gamma}_\nu\bar{P}_\nu{}^2\pi_\lambda(1+\bar{P}_\lambda)\left(\frac{2\bar{\gamma}_\nu\bar{P}_\nu}{-i\omega+\bar{\gamma}_\nu}+1\right)\left(i\omega+\bar{\Gamma}_2+\sum_{\mu\neq\nu}{}' \frac{\pi_\mu\gamma_\mu\bar{P}_\mu}{i\omega+\bar{\gamma}_\mu}\right)-\bar{\gamma}_\lambda\bar{P}_\lambda{}^2\pi_\nu(1+\bar{P}_\nu)\left(\frac{2\bar{\gamma}_\lambda\bar{P}_\lambda}{i\omega+\bar{\gamma}_\lambda}+1\right)\right.$$

$$\left.\times\left(-i\omega+\bar{\Gamma}_2+\sum_{\mu\neq\lambda}{}' \frac{\pi_\mu\gamma_\mu\bar{P}_\mu}{-i\omega+\bar{\gamma}_\mu}\right)+\gamma_\lambda\bar{P}_\lambda\gamma_\nu\bar{P}_\nu\left(\frac{\pi_\lambda{}^2\bar{P}_\lambda}{i\omega+\bar{\gamma}_\lambda}+\frac{\pi_\nu{}^2\bar{P}_\nu}{-i\omega+\bar{\gamma}_\nu}+2\sum_{\mu\neq\lambda,\nu}{}'' \frac{\pi_\mu{}^2\gamma_\mu\bar{P}_\mu}{\omega^2+\bar{\gamma}_\mu{}^2}\right)\right\}. \quad (4.20b)$$

These functions have the property $\Delta P_{\lambda\nu}(-\omega)=\Delta P_{\nu\lambda}(\omega)$ required by the time symmetry (4.11). The expression (4.20a) reduces to (2.23) when only one photon mode is significant.

Only photon modes for which there is significant stimulated emission need be explicitly included in the preceding calculation. The effect of all other modes can be absorbed in the relaxation rate Γ_2.[42]

An important special case is that for which all lasing modes have identical parameters

$$\pi_\lambda=\pi_0, \quad \gamma_\lambda=\gamma, \quad \bar{P}_\lambda=\bar{P}. \quad (4.21)$$

If in this case there are m lasing modes, Eqs. (4.20) become

$$\Delta P_{\lambda\lambda}(\omega)_Q=\frac{2\bar{\gamma}\bar{P}^2\{[\bar{\Gamma}_2\bar{\gamma}+(m-1)\pi_0\gamma\bar{P}-\omega^2]^2+\omega^2(\bar{\gamma}+\bar{\Gamma}_2)^2+(m-1)\pi_0{}^2\gamma^2\bar{P}^2-\pi_0(1+\bar{P})\bar{\Gamma}_2(\omega^2+\bar{\gamma}^2)\}}{(\omega^2+\bar{\gamma}^2)\{[\bar{\Gamma}_2\bar{\gamma}+m\pi_0\gamma\bar{P}-\omega^2]^2+\omega^2(\bar{\gamma}+\bar{\Gamma}_2)^2\}} \quad (4.22a)$$

and for $\lambda \neq \nu$

$$\Delta P_{\lambda\nu}(\omega)_Q=\frac{-2\bar{\gamma}\bar{P}^2\{2\pi_0\gamma\bar{P}(\bar{\gamma}\bar{\Gamma}_2-\omega^2)+m(\pi_0\gamma\bar{P})^2+\pi_0(1+\bar{P})\bar{\Gamma}_2(\omega^2+\bar{\gamma}^2)\}}{(\omega^2+\bar{\gamma}^2)\{[\bar{\Gamma}_2\bar{\gamma}+m\pi_0\gamma\bar{P}-\omega^2]^2+\omega^2(\bar{\gamma}+\bar{\Gamma}_2)^2\}}. \quad (4.22b)$$

For $m\geq 2$ these expressions differ significantly from the single-mode expression (2.23) and from the power spectrum describing fluctuations in the total photon output $P_{TO}=\sum_\lambda \gamma_\lambda P_\lambda$, especially in their low-frequency behavior when $\bar{\gamma}\to 0$ ($\bar{P}\to\infty$). For the case (4.21) the power spectrum describing the fluctuations in the photon output of $n\leq m$ modes is[43]

$$\Delta P(\omega)_Q\Big|_{\substack{n \text{ of } m\\ \text{modes}}}=\sum_{\lambda\mu}\gamma_\lambda\gamma_\mu\Delta P_{\lambda\mu}(\omega)_Q\Big|_{\substack{\lambda\mu \text{ sum over}\\ n \text{ of } m \text{ modes}}} \quad (4.23a)$$

$$=\frac{2n\bar{\gamma}\bar{P}^2\{(\omega^2+\bar{\Gamma}_2[\bar{\Gamma}_2-n\pi_0(1+\bar{P})])+(m-n)[2\pi_0\gamma\bar{P}(\bar{\Gamma}_2\bar{\gamma}-\omega^2)+m(\pi_0\gamma\bar{P})^2]/(\omega^2+\bar{\gamma}^2)\}}{[\bar{\Gamma}_2\bar{\gamma}+m\pi_0\gamma\bar{P}-\omega^2]^2+\omega^2(\bar{\gamma}+\bar{\Gamma}_2)^2}. \quad (4.23b)$$

When $n=m$, this has the form (2.23) of the single-mode power spectrum. Note that when the output from all modes is detected ($n=m$), the power spectrum (4.23) does *not* have the "weak pump" $(\omega^2+\bar{\gamma}^2)^{-1}$ behavior [compare Eqs. (2.25)] present in (4.22).

These expressions illustrate an important general result. When one or more modes are strongly pumped, the nonlinearity inherent in the rate-equations (4.3) stabilizes the quantum fluctuations in the *total* rate of photon output but does *not* stabilize the output of individual modes. For example, the low-frequency divergence in Eqs. (4.22) and (4.23) when $\bar{\gamma}\to 0$ ($\bar{P}\to\infty$) results from fluctuations in the partition of the total output between different strongly pumped modes.

A more detailed discussion of fluctuations in multimode lasers will be given elsewhere.

5. INTERMEDIATE ATOMIC PUMPING LEVELS

A careful inspection of Eqs. (2.1) and (4.3) and of Fig. 1 will reveal that the pumping rate $R(t)$ used in those equations represents the rate at which atoms are

[42] Because Γ_2 appears in the final spectra (4.19) and (4.20) only through $\bar{\Gamma}_2$ and because $\bar{\Gamma}_2$ in Eqs. (2.12) and (4.8a) includes radiative relaxation, it is clear that Γ_2 should include all upper-laser-level relaxation processes not explicitly included elsewhere in the rate-equations. [The Γ_2 in the numerator of (2.23) is more appropriately written $\bar{\Gamma}_2-\pi_\lambda(1+\bar{P}_\lambda)$, the expression ppearing in the numerator of (4.20a).]

[43] The intensity spectrum measured by allowing the output from several modes to fall on the same photomultiplier will contain contributions from the beat spectra (4.13) as well as the spectra (4.22). However, if, as is often the case, the optical beat frequencies are much larger than the fluctuation frequencies of interest, the beat spectra (4.13) can be neglected.

excited to the upper-laser level 2 and that $R(t)$ is only indirectly related to the strength $R_e(t)$ of the actual external pumping field which excites ground-state atoms to the intermediate pumping level 3. In this section we consider how $R(t)$ relates to $R_e(t)$ and show that additional shot noise does not result from level-3 to level-2 transitions. It is sufficient for these purposes to consider the single-mode system of Sec. 2, extending Eqs. (2.1) to include the level-3 population $N_3(t)$.

Assuming that transitions from level 3 to lower levels $j=0$ and 2 are described by relaxation rates w_{j3} and assuming as before that $N_1(t)=0$, we take in place of Eqs. (2.1)

$$(\partial/\partial t)N_3(t)=r_3(t)+R_e(t)-(w_{03}+w_{23})N_3(t), \tag{5.1a}$$

$$(\partial/\partial t)N_2(t)=r_2(t)+w_{23}N_3(t)-\Gamma_2N_2(t) -\pi_\lambda[1+P_\lambda(t)]N_2(t), \tag{5.1b}$$

$$(\partial/\partial t)P_\lambda(t)=s(t)+\pi_\lambda[+P_\lambda(t)]N_2(t)-\gamma_\lambda P_\lambda(t). \tag{5.1c}$$

Here $s(t)$, $r_2(t)$, and $r_3(t)$ are fictitious noise signals which reproduce the intrinsic quantum fluctuations (Sec. 3) and $R_e(t)$ is the rate at which atoms are excited by the external pump to level 3. In steady state the average populations satisfy [compare Eqs. (2.2)]

$$\begin{aligned}\bar{R}_e&=(w_{03}+w_{23})\bar{N}_3,\\ w_{23}\bar{N}_3&=\Gamma_2\bar{N}_2+\pi_\lambda(1+\bar{P}_\lambda)\bar{N}_2,\\ \gamma_\lambda\bar{P}_\lambda&=\pi_\lambda(1+\bar{P}_\lambda)\bar{N}_2.\end{aligned} \tag{5.2}$$

The linear equations describing small fluctuations about these average values are [compare Eqs. (2.3) and (2.12)]

$$(\partial/\partial t)n_3(t)=r_3(t)+r_e(t)-(w_{03}+w_{23})n_3(t), \tag{5.3a}$$

$$(\partial/\partial t)n_2(t)=r_2(t)+w_{23}n_3(t) -\bar{\Gamma}_2n_2(t)-\pi_\lambda\bar{N}_2p_\lambda(t), \tag{5.3b}$$

$$(\partial/\partial t)p_\lambda(t)=s(t)+\pi_\lambda(1+\bar{P}_\lambda)n_2(t)-\bar{\gamma}_\lambda p_\lambda(t). \tag{5.3c}$$

Using these equations to compute the photon power spectrum by the method outlined in the preceding sections, we find

$$\Delta P_{\lambda\lambda}(\omega)=\frac{\pi_\lambda^2(1+\bar{P}_\lambda)^2\{w_{23}^2\Delta P_{RR}(\omega)_e/[\omega^2+(w_{03}+w_{23})^2]\}+2\bar{\gamma}_\lambda\bar{P}_\lambda^2(\omega^2+\bar{\Gamma}_2\Gamma_2)}{(\bar{\gamma}_\lambda\bar{\Gamma}_2+\pi_\lambda\gamma_\lambda\bar{P}_\lambda-\omega^2)^2+\omega^2(\bar{\Gamma}_2+\bar{\gamma}_\lambda)^2}, \tag{5.4}$$

where

$$\Delta P_{RR}(\omega)_e=\int_{-\infty}^{\infty}d\tau\, e^{i\omega\tau}\langle r_e(t+\tau)r_e(t)\rangle_t \tag{5.5}$$

is the power spectrum of the external pumping signal. Comparing Eq. (5.4) with Eqs. (2.16) and (2.23), we see that the result (5.4) is identical to that obtained before if we set

$$\Delta P_{RR}(\omega)=(w_{23}^2/[\omega^2+(w_{03}+w_{23})^2])\Delta P_{RR}(\omega)_e. \tag{5.6}$$

This same power spectrum would obtain if the signal $r(t)$ was obtained by passing $r_e(t)$ through a filter with transfer function

$$y_{23}(\omega)=w_{23}/(w_{03}+w_{23}-i\omega). \tag{5.7}$$

Because this is precisely the transfer function predicted from Eq. (5.3a) if $r(t)=w_{23}n_3(t)$, a choice consistent with Eqs. (2.3a) and (5.3b), we conclude that for any given external pumping signal the results of the preceding sections correctly represent all intrinsic quantum fluctuations and all bona-fide pump fluctuations provided only that in Eqs. (2.16) and (4.19)

$$\Delta P_{RR}(\omega)=|Y(\omega)|^2\Delta P_{RR}(\omega)_e, \tag{5.8}$$

where $Y(\omega)$ is the transfer function describing how bona-fide pump fluctuations $r_e(t)$, exclusive of quantum noise, are reflected in the rate at which atoms are excited to the upper laser level.

6. CONCLUDING REMARKS AND EXAMPLES

In the preceding sections we used rate-equations to compute population power spectra of four-level lasers in which the lower-level population $N_1(t)\approx 0$. These spectra pertain to the intensity fluctuations in the output of cw laser oscillators as measured by apparatus described in the Introduction. Such fluctuations stem from two distinct sources: (i) quantum shot noise intrinsic to the laser and (ii) random external fields perturbing the laser. The physical origin of the quantum noise is discussed in detail in Secs. 2 and 3; briefly, it arises because atomic and photon populations are characterized by integral quantum numbers, not by continuous variables. The importance of external perturbing fields depends to a large extent upon the environment of the laser and upon the method used for atomic pumping.[44]

In Table I we have listed parameters typical of some

TABLE I. Typical laser parameters.

	Gas laser	Solid laser	Solid-state diode laser
$\Gamma_2(\text{sec}^{-1})$	10^8	10^3	10^9
$\pi_\lambda(\text{sec}^{-1})$	10^{-1}	10^{-6}	10^5
$\gamma_\lambda(\text{sec}^{-1})$	10^7	10^9	10^{11}

[44] L. J. Prescott and A. Van der Ziel, Appl. Phys. Letters **5**, 48 (1964); J. A. Collinson (to be published).

gas (volume ~ 100 cc), solid (volume ~ 1 cc), and solid-state diode (volume $\sim 10^{-8}$ cc) lasers. We have taken Γ_2 equal to a typical rate of spontaneous radiative relaxation of the upper laser level[42] and have used Kleinman's Eq. (7) with this rate and typical inhomogeneous linewidths to compute π_λ.[32] Using these parameters in the expressions of Sec. 2, we have computed the intensity-fluctuation properties of these typical lasers in single-mode operation. As we showed in Sec. 4, qualitatively similar results pertain to the *total* output of multimode devices.

Considering first the intrinsic quantum fluctuations, we have plotted in Fig. 2 the dimensionless ratio[34] [compare Eqs. (2.7) and (2.24); notation defined in Eqs. (2.1)–(2.3) and (2.12)]

$$\Delta C_I(0)_Q/C_I(\infty)=\frac{\bar{\gamma}_\lambda(\bar{\Gamma}_2\Gamma_2+\bar{\gamma}_\lambda\bar{\Gamma}_2+\pi_\lambda\gamma_\lambda\bar{P}_\lambda)}{(\bar{\Gamma}_2+\bar{\gamma}_\lambda)(\bar{\gamma}_\lambda\bar{\Gamma}_2+\pi_\lambda\gamma_\lambda\bar{P}_\lambda)} \quad (6.1)$$

as a function of the average photon population $\bar{P}_\lambda$. This ratio is a measure of the relative mean-squared intensity fluctuations (summed over all frequencies) and is pertinent, for example, to the $\tau=0$ HB&T measurement (1.12) and to the high-resolution coincidence measurement (1.15b).[45] Of particular importance is the fact that these fluctuations are always less than (or equal to) those predicted by the approximate expression (2.25b) for weak pumping

$$\Delta C_I(0)_Q/C_I(\infty)\big|_{\substack{\text{weak}\\ \text{pump}}}=1. \quad (6.2)$$

The latter large fluctuations would obtain if the laser

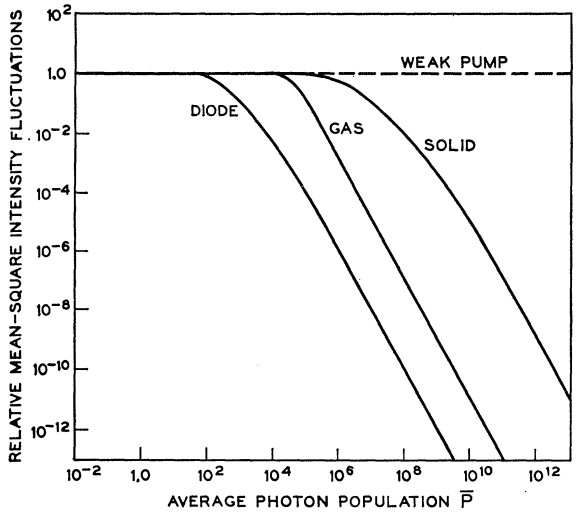

FIG. 2. Relative intensity fluctuations $\Delta C_I(0)_Q/C_I(\infty)$ versus average photon population $\bar{P}_\lambda$ for the lasers of Table I. The solid curves represent the function (6.1), the dashed curve the approximation (6.2) appropriate to weak pumping.

[45] While the relative fluctuations (6.1) *decrease* monotonically with $\bar{P}_\lambda$ (Fig. 2), the absolute fluctuations $\Delta C_{\lambda\lambda}(0)_Q$ *increase* monotonically with $\bar{P}_\lambda$.

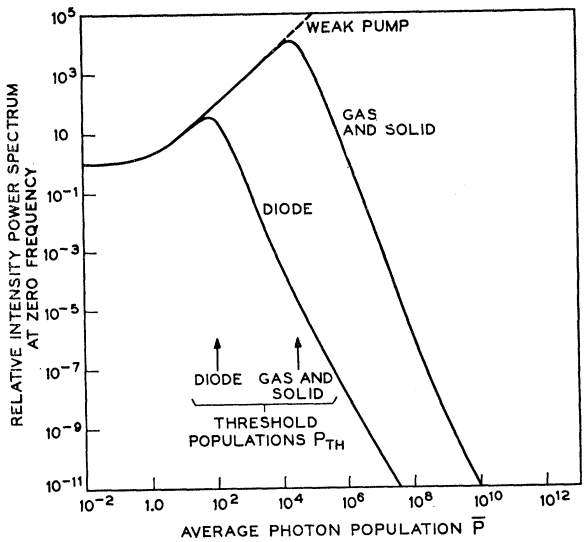

FIG. 3. Normalized power spectrum at zero frequency of intensity fluctuations $\frac{1}{2}\gamma_\lambda\Delta P_I(\omega)_Q/C_I(\infty)$ versus average photon population $\bar{P}_\lambda$ for lasers of Table I. The solid curves represent the function (6.3), the dashed curve the approximation (6.4) appropriate to weak pumping. These curves equivalently give [compare Eq. (6.3)] the correlation time τ_I defined in Eq. (1.14).

operated as a noise amplifier with fixed gain.[46] In fact, the gain is not constant but depends dynamically upon the photon population $P_\lambda(t)$; the dynamic feedback (saturation) stabilizes the intensity fluctuations.[36]

This stabilization is most effective at low frequencies where the atomic population inversion can respond to the photon fluctuations. In Fig. 3 we have plotted the zero-frequency spectral density[34] [compare Eqs. (1.10), (1.14), and (2.23)]

$$\tfrac{1}{2}\gamma_\lambda\Delta P_I(0)_Q/C_I(\infty)=\tfrac{1}{2}\gamma_\lambda\tau_I$$
$$=\gamma_\lambda\bar{\gamma}_\lambda\Gamma_2\bar{\Gamma}_2/(\bar{\gamma}_\lambda\bar{\Gamma}_2+\pi_\lambda\gamma_\lambda\bar{P}_\lambda)^2 \quad (6.3)$$

as a function of $\bar{P}_\lambda$. The correlation time τ_I is relevant to the low-resolution coincidence measurements of Eq. (1.15a). Because $\bar{\gamma}_\lambda=\gamma_\lambda/(1+\bar{P}_\lambda)$, the ratio (6.3) is independent of γ_λ. Here, as before, the weak-pump approximation

$$\tfrac{1}{2}\gamma_\lambda\Delta P_I(0)_Q/C_I(\infty)\big|_{\substack{\text{weak}\\ \text{pump}}}=(1+\bar{P}_\lambda), \quad (6.4)$$

based upon Eq. (2.25a), overestimates the low-frequency fluctuations.

In Fig. 3 the relative low-frequency intensity fluctuations increase with photon population $\bar{P}_\lambda>1$ until they reach a maximum near the threshold value[47]

$$\bar{P}_{\text{th}}=(\bar{\Gamma}_2/\pi_\lambda)^{1/2}\gg 1 \quad (6.5)$$

[46] E. I. Gordon, Bell System Tech. J. 43, 507 (1964).

[47] The corresponding threshold pumping rate is $\bar{R}_{\text{th}}=\bar{\Gamma}_2\gamma_\lambda\bar{P}_\lambda/\pi_\lambda(1+\bar{P}_\lambda)\approx\Gamma_2\gamma_\lambda/\pi_\lambda$ if $\bar{\Gamma}_2/\pi_\lambda\gg 1$, as it generally is in practice. The approximate form is equivalent to the familiar Schawlow-Townes criterion [A. L. Schawlow and C. H. Townes, Phys. Rev. 112, 1940 (1959)]; however, it is less useful to us than the criterion (6.5) because $\bar{P}_\lambda$ is extremely sensitive to very small fractional changes in $\bar{R}$ for $\bar{R}\approx\bar{R}_{\text{th}}$.

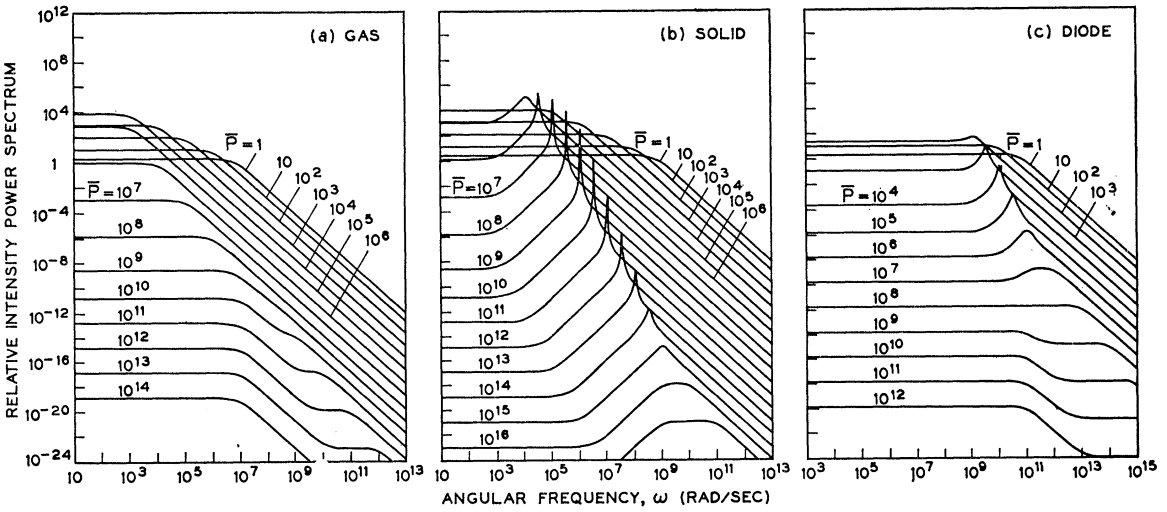

FIG. 4. Power spectrum of relative intensity fluctuations $\frac{1}{2}\gamma_\lambda \Delta P_I(\omega)_Q/C_I(\infty)$ versus angular frequency ω for different average populations $\bar{P}_\lambda$ for the lasers of Table I: (a) gas laser, (b) solid laser, and (c) solid-state diode laser. Low-frequency values agree with Fig. 3. The curves for very small and for very large $\bar{P}_\lambda$ are qualitatively similar for all lasers. For intermediate $\bar{P}_\lambda$ values, the solid-state lasers differ from the gas laser in that they exhibit sharp increases in noise at resonance frequencies lying just below the high-frequency cutoffs.

of the photon population for which $\bar{\Gamma}_2\bar{\gamma}_\lambda = \pi_\lambda\gamma_\lambda P_\lambda$, the boundary of the weak-pump and strong-pump regions of Sec. 2. Above this threshold, stabilization is effective, and the relative fluctuations decrease rapidly with increasing $\bar{P}_\lambda$. Below threshold the fluctuations follow the weak-pump expressions. The threshold (6.5) is also the population level at which a finite fraction $(\frac{1}{2})$ of any incremental increase $\Delta\bar{R}$ in pumping rate $\bar{R}$ is reflected in the laser-mode output. Well below threshold $\gamma_\lambda \Delta\bar{P}_\lambda/\Delta\bar{R} \simeq 0$; well above threshold $\gamma_\lambda \Delta\bar{P}_\lambda/\Delta\bar{R} \approx 1$.

Spectral distributions of the intrinsic quantum intensity fluctuations are indicated in detail in Fig. 4. There we have plotted the relative power spectrum[34] [compare Eq. (2.23)]

$$\frac{\frac{1}{2}\gamma_\lambda \Delta P_I(\omega)_Q/C_I(\infty)}{} = \frac{\gamma_\lambda^2(\omega^2+\Gamma_2\bar{\Gamma}_2)/(1+\bar{P}_\lambda)}{(\bar{\gamma}_\lambda\bar{\Gamma}_2+\pi_\lambda\gamma_\lambda\bar{P}_\lambda-\omega^2)^2+\omega^2(\bar{\Gamma}_2+\bar{\gamma}_\lambda)^2} \tag{6.6}$$

as a function of angular frequency ω for different values $\bar{P}_\lambda$. This expression is relevant to the single-detector measurements of Eqs. (1.17) and (1.19). The low-frequency values in Fig. 4 are consistent with Fig. 3.

The parameters for the gas laser of Table I are such $(\bar{\Gamma}_2 \gg \gamma_\lambda)$ that the function (6.6) remains nearly constant at its $\omega=0$ value for all $\omega^2 < \omega_c^2$, where

$$\omega_c^2 \equiv (\bar{\gamma}_\lambda + \pi_\lambda\gamma_\lambda\bar{P}_\lambda/\bar{\Gamma}_2)^2 \tag{6.7a}$$

$$\xrightarrow[\bar{P}_\lambda < \bar{P}_{\rm th}]{} \gamma_\lambda^2/(1+\bar{P}_\lambda)^2 \tag{6.7b}$$

$$\xrightarrow[\bar{P}_\lambda > \bar{P}_{\rm th}]{} \gamma_\lambda^2\bar{P}_\lambda^2/(\bar{P}_{\rm th}^2+\bar{P}_\lambda)^2. \tag{6.7c}$$

For $\omega^2 > \omega_c^2$ the function (6.6) decreases as $\gamma_\lambda^2/\omega^2(1+\bar{P}_\lambda)$, to within the factor $(\omega^2+\Gamma_2\bar{\Gamma}_2)/(\omega^2+\bar{\Gamma}_2^2)$ which is different from unity only for $\bar{P}_\lambda \gtrsim \bar{P}_{\rm th}$.[48] For very small and for very large populations $\bar{P}_\lambda$ the solid-state-laser spectra are similar in their general features to the gas-laser spectra of Fig. 4(a). However, for a broad range of important intermediate $\bar{P}_\lambda$ values the solid-state spectra are qualitatively different. Superimposed upon the expected smooth background are strong anomalous noise

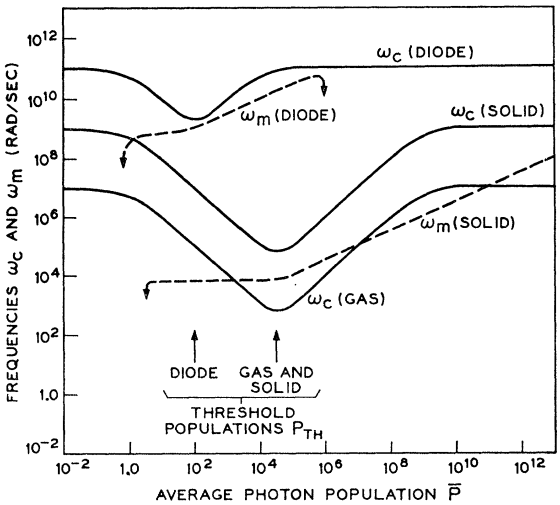

FIG. 5. Frequencies ω_c (solid lines) and ω_n (dashed lines) versus phonon population $\bar{P}_\lambda$ for the lasers of Table I. Values of ω_m are only indicated for those $\bar{P}_\lambda$ such that $\omega_m^2 > 0$; this condition never obtains in the gas laser. At the ends of the indicated ω_m curves, ω_m falls abruptly to zero.

[48] Recall that at extremely high frequencies our results are invalid because the rate-equations upon which they are based no longer obtain.

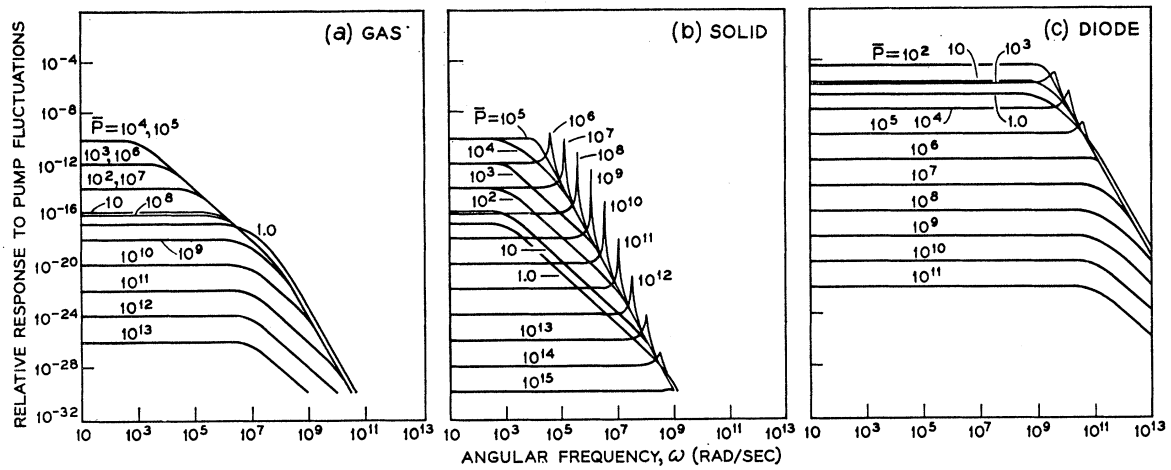

FIG. 6. Relative response $\gamma_\lambda^2[\Delta P_I(\omega)/C_I(\infty)]/\Delta P_{RR}(\omega)$ of the lasers of Table I to pump-fluctuation noise versus the angular frequency ω of that noise: (a) gas laser, (b) solid laser, and (c) solid-state diode laser. The different curves belong to different values of the population $\bar{P}_\lambda$.

peaks near the high-frequency "spiking" resonances of the laser.[49]

The function (6.6) has an extremum at $\omega=0$ and, if

$$\omega_m^2 \equiv -\Gamma_2\bar{\Gamma}_2+\{[\bar{\Gamma}_2(\Gamma_2+\bar{\gamma}_\lambda)+\pi_\lambda\gamma_\lambda\bar{P}_\lambda]^2 -\Gamma_2\bar{\Gamma}_2(\bar{\Gamma}_2+\bar{\gamma}_\lambda)^2\}^{1/2}>0, \quad (6.8)$$

it has maxima at $\omega=\pm\omega_m$. (If $\omega_m^2<0$, $\omega=0$ is the only maximum; if $\omega_m^2>0$, $\omega=0$ is a minimum.) The condition $\omega_m^2>0$ never obtains in any laser when $\bar{P}_\lambda=0$ or when $\bar{P}_\lambda\gg\bar{P}_{\rm np}\equiv\max(\Gamma_2/\pi_\lambda,\gamma_\lambda/\pi_\lambda)$, facts which account for the qualitative similarity of all spectra (6.6) at the extremes of small and large $\bar{P}_\lambda$ values

$$\tfrac{1}{2}\gamma_\lambda\Delta P_I(\omega)_Q/C_I(\infty) \xrightarrow[\bar{P}_\lambda\leq\bar{P}_{\rm th}]{} \gamma_\lambda^2/(\omega^2+\omega_c^2)(1+\bar{P}_\lambda) \quad (6.9a)$$

$$\xrightarrow[\bar{P}_\lambda>>\bar{P}_{\rm np}]{} \gamma_\lambda^2/(\omega^2+\gamma_\lambda^2)\bar{P}_\lambda. \quad (6.9b)$$

The requirement $\omega_m^2>0$ is not met for any population $\bar{P}_\lambda$ in the gas laser; however, it is met for some $\bar{P}_\lambda$ in the solid-state lasers.

In the pumping range for which the anomalous peaks are strong and sharp, the amplitude fluctuation noise (6.1) is predominantly concentrated in those peaks. However, notice that the anomalous ω_m peaks do not influence the correlation time τ_I defined in Eq. (6.3) and that their noise contributions are not relevant to the low-resolution coincidence measurements of Eq. (1.15a).

In Fig. 5 we have plotted the cutoff frequency ω_c of Eq. (6.7) as a function of $\bar{P}_\lambda$. Note the dip in ω_c at $\bar{P}_\lambda=\bar{P}_{\rm th}$. For the solid-state lasers we have included in Fig. 5 plots of ω_m for those $\bar{P}_\lambda$ values for which $\omega_m^2>0$.

In Fig. 6 we have indicated how the lasers of Table I respond to bona-fide pump fluctuations.[44] We have plotted [compare Eq. (2.16)]

$$\frac{\gamma_\lambda^2}{\Delta P_{RR}(\omega)}\frac{\Delta P_I(\omega)_{RS}}{C_I(\infty)} = \frac{[\pi_\lambda\gamma_\lambda(1+\bar{P}_\lambda)/\bar{P}_\lambda]^2}{(\bar{\gamma}_\lambda\bar{\Gamma}_2+\pi_\lambda\gamma_\lambda\bar{P}_\lambda-\omega^2)^2+\omega^2(\bar{\Gamma}_2+\bar{\gamma}_\lambda)^2} \quad (6.10)$$

as a function of angular frequency ω for different values of $\bar{P}_\lambda$. Here $\Delta P_{RR}(\omega)$ is the pump-noise power spectrum of Eq. (5.8). As in Fig. 4, the different lasers are qualitatively similar at the extremes of very weak and very strong pumping; however, the solid-state lasers differ in the intermediate pumping region through the appearance of spiking resonances near the frequencies $\pm\omega_m$.[49] These resonances appear at frequencies $\omega=\pm\omega_r$ when

$$\omega_r^2\equiv\pi_\lambda\gamma_\lambda\bar{P}_\lambda-\tfrac{1}{2}(\bar{\Gamma}_2^2+\bar{\gamma}_\lambda^2) \quad (6.11)$$

is positive. The conditions for which $\omega_r^2>0$ are similar to those for which $\omega_m^2>0$.

In testing the high-frequency predictions of the theory of this paper,[48] it may prove useful to modulate the laser output intensity by modulating the cavity loss parameter γ_λ. This is equivalent in Eqs. (2.1) to introducing an external signal

$$s(t)=-\bar{P}_\lambda\delta\gamma_\lambda(t). \quad (6.12)$$

If the modulation has the time dependence

$$\delta\gamma_\lambda(t)=\xi\gamma_\lambda\cos\omega_0 t, \quad (6.13)$$

where the relative modulation ξ is sufficiently small that a linear analysis applies, it follows from the equations of Sec. 2 that the relative modulation of the photon in-

[49] Cf. Ref. 32, especially Eq. (56) ff, and the references cited therein.

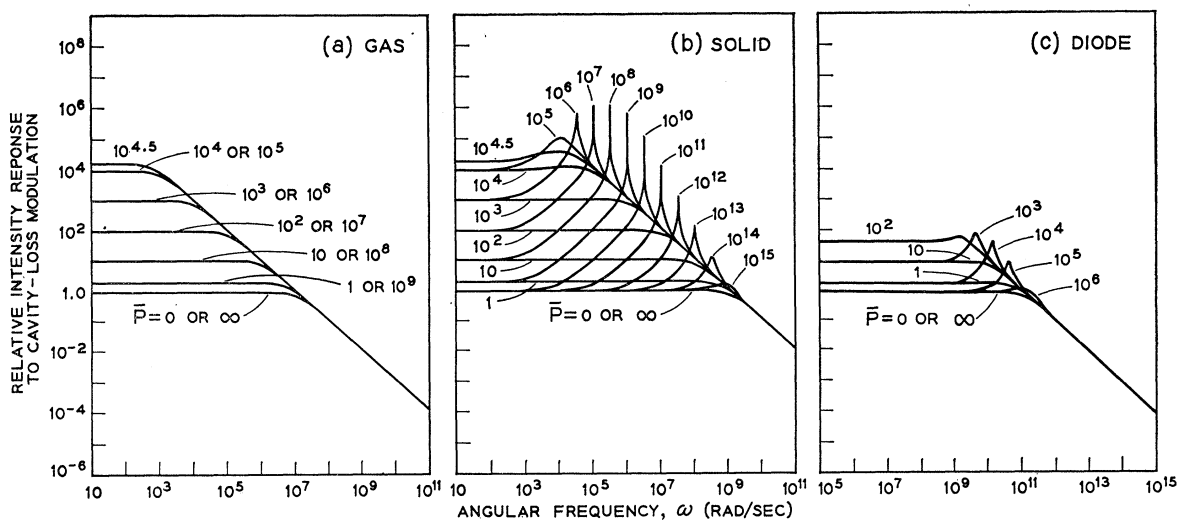

FIG. 7. Magnitude $M_\lambda(\omega)$ of the relative response of photon intensity in the lasers of Table I to modulation of the cavity loss parameter γ_λ versus the angular frequency ω of that modulation: (a) gas laser, (b) solid laser, and (c) solid-state diode laser. The different curves belong to different values of the population $\bar{P}_\lambda$.

tensity is

$$\delta P_\lambda(t)/\bar{P}_\lambda = -\xi M_\lambda(\omega_0)\cos[\omega_0 t - \delta_\lambda(\omega_0)], \quad (6.14)$$

where

$$M_\lambda(\omega) = \left\{\frac{\gamma_\lambda^2(\omega^2+\bar{\Gamma}_2^2)}{(\bar{\gamma}_\lambda\bar{\Gamma}_2+\pi_\lambda\gamma_\lambda\bar{P}_\lambda-\omega^2)^2+\omega^2(\bar{\Gamma}_2+\bar{\gamma}_\lambda)^2}\right\}^{1/2} \quad (6.15a)$$

and

$$\delta_\lambda(\omega) = \text{Arctan}\left\{\frac{\omega(\bar{\Gamma}_2^2-\pi_\lambda\gamma_\lambda\bar{P}_\lambda+\omega^2)}{\bar{\Gamma}_2^2\bar{\gamma}+\bar{\Gamma}_2\pi_\lambda\gamma_\lambda\bar{P}_\lambda+\omega^2\bar{\gamma}_\lambda}\right\}. \quad (6.15b)$$

The modulation function $M_\lambda(\omega)$ has been plotted in Fig. 7 for the three lasers of Table I. The curves show many similarities to those of Figs. 4 and 6. Note in particular the resonance peaks at $\omega=\pm\omega_M$ for the solid-state systems when

$$\omega_M^2 \equiv -\bar{\Gamma}_2^2+\{[\bar{\Gamma}_2(\bar{\Gamma}_2+\bar{\gamma}_\lambda)+\pi_\lambda\gamma_\lambda\bar{P}_\lambda]^2 - \bar{\Gamma}_2^2(\bar{\Gamma}_2+\bar{\gamma}_\lambda)^2\}^{1/2} \quad (6.16)$$

is positive.

We shall not endeavor to compare our results in detail with measurements of intensity fluctuation noise in lasers near threshold until after we report in Paper II the generalizations appropriate to finite occupation of the lower laser level ($N_1\neq 0$).[50] However, we should remark that the intensity-fluctuation measurements reported to date are in excellent agreement with the theory described above. Prescott and Van der Ziel[24] measured the output spectrum of a photon counter in that frequency range where the intrinsic laser noise exceeds the counter shot noise; their results for the He-Ne gas laser are qualitatively consistent with the spectra of Fig. 4(a). More recent gas-laser measurements by Freed and Haus[6] are in quantitative agreement with our theory, as are the measurements of Geusic[7] for the solid YAlG:Nd laser. Geusic's measurements show the spiking resonance peak expected in the solid system and shown in Fig. 4(b). A similar resonance peak has been seen in the ruby microwave maser by Bloembergen and Dimitrewsky.[8] Armstrong and Smith[22,23] used low-resolution[51] coincidence techniques to study the GaAs diode laser; their measurements of τ_I of Eq. (1.16a) are quantitatively consistent with Eq. (6.3) and Fig. 3, to within the accuracy of the parameters of Table I. Multimode effects consistent with the predictions of Sec. 4 have also been observed in the solid[7] and diode[23] lasers.

ACKNOWLEDGMENTS

I am grateful to C. G. B. Garrett, D. A. Kleinman, and M. Lax for a number of helpful suggestions; I also wish to acknowledge conversations, in the course of preparing this paper, with J. A. Armstrong, J. A. Collinson, W. L. Faust, E. I. Gordon, R. A. McFarlane, and H. Seidel.

[50] It can be shown that, as the rate of decay from the lower-laser level increases toward infinity and $\bar{N}_1 \to 0$, the finite-$\bar{N}_1$ four-level-laser expressions reduce to those derived above.

[51] If τ_R is the coincidence resolving time, measurements have "low resolution" if $\tau_R\omega \gg 1$ for the appropriate $\bar{P}_\lambda$ values. In the diode laser above threshold (compare Fig. 5) $\omega_m \sim \omega_c \geq 10^9$ sec$^{-1} \gg \tau_R^{-1} = 2\times 10^8$ sec^{-1} for the Armstrong and Smith resolving time $\tau_R = 5\times 10^{-9}$ sec.